SCIENCE TRANSLATIONAL MEDICINE | RESEARCH ARTICLE

BONE

Osteoclast-mediated bone resorption is controlled by a compensatory network of secreted and membrane-tethered metalloproteinases

Lingxin Zhu[1,2,3]*, Yi Tang[2,3], Xiao-Yan Li[2,3], Evan T. Keller[4], Jingwen Yang[1,5], Jung-Sun Cho[2,3], Tamar Y. Feinberg[2,3], Stephen J. Weiss[2,3]*

Osteoclasts actively remodel both the mineral and proteinaceous components of bone during normal growth and development as well as pathologic states ranging from osteoporosis to bone metastasis. The cysteine proteinase cathepsin K confers osteoclasts with potent type I collagenolytic activity; however, cathepsin K–null mice, as well as cathepsin K–mutant humans, continue to remodel bone and degrade collagen by as-yet-undefined effectors. Here, we identify a cathepsin K–independent collagenolytic system in osteoclasts that is composed of a functionally redundant network of the secreted matrix metalloproteinase MMP9 and the membrane-anchored matrix metalloproteinase MMP14. Unexpectedly, whereas deleting either of the proteinases individually leaves bone resorption intact, dual targeting of *Mmp9* and *Mmp14* inhibited the resorptive activity of mouse osteoclasts in vitro and in vivo and human osteoclasts in vitro. In vivo, *Mmp9*/*Mmp14* conditional double-knockout mice exhibited marked increases in bone density and displayed a highly protected status against either parathyroid hormone– or ovariectomy-induced pathologic bone loss. Together, these studies characterize a collagenolytic system operative in mouse and human osteoclasts and identify the MMP9/MMP14 axis as a potential target for therapeutic interventions for bone-wasting disease states.

INTRODUCTION

Bone mass is maintained by coordinating the activity of bone-resorbing osteoclasts with bone-forming osteoblasts (*1*–*4*). Accordingly, an imbalance of bone remodeling arising as a consequence of increased osteoclast activity leads to bone-wasting states in diseases ranging from osteoporosis and rheumatoid arthritis to periodontitis and bone metastasis (*1*–*3*). Because patients with osteoclast-related diseases are at higher risk of bone fractures with its attendant morbidity, the associated economic burden is a serious public health issue (*5*, *6*). Nevertheless, despite the development of several antiresorptive therapeutics, their efficiency and long-term bone-sparing effects remain unclear, and their use can be undermined by arrested bone remodeling and unanticipated side effects (*5*, *6*). Hence, elucidating the molecular mechanisms that underlie osteoclast activity will not only further enhance our understanding of the pathogenesis of bone-wasting disorders but also provide new potential targets for therapeutic intervention.

In response to the cytokines macrophage colony-stimulating factor (M-CSF) and receptor activator of nuclear factor κB ligand (RANKL), monocyte precursors differentiate into bone marrow–derived macrophages (BMDMs) that ultimately fuse to form multinucleated polykaryons, osteoclasts (*2*–*4*). Upon attachment to bone, osteoclasts polarize and undergo extensive morphologic changes to form an actin ring that circumscribes a bone resorptive microenvironment, termed the sealing zone (*2*–*4*). In turn, the sealing zone surrounds the ruffled border, a differentiated region of the plasma membrane where protons, chloride ions, and various enzymes are delivered into the resorption lacuna (*2*–*4*). Coincident with this process, osteoclasts mobilize proteinases whose functions are most commonly linked to the degradation of triple-helical type I collagen, the dominant extracellular matrix (ECM) component found in the bone (*1*). Cathepsin K (CTSK), a cysteine proteinase that is highly expressed in osteoclasts, has long been assumed to play a dominant, if not exclusive, role in bone ECM degradation, because it is one of the few enzymes in the mammalian genome capable of degrading native type I collagen (*7*–*10*). However, studies of humans with pycnodysostosis who are *CTSK* deficient, as well as *Ctsk* knockout mice, demonstrate that considerable bone remodeling activity is maintained in the absence of this proteinase (*11*–*13*). Consistent with these findings, large quantities of collagen fragments accumulate within the lysosomal compartments of osteoclasts found in either *Ctsk*-null mice or humans with *CTSK* mutations (*14*, *15*).

In considering alternate collagenolytic systems, osteoclasts are known to express several secreted and membrane-anchored members of the matrix metalloproteinase (MMP) family (*16*, *17*). Although several members of this MMP family express type I collagenolytic activity in vitro (MMP8, MMP13, and MMP14), global knockout of each of these enzymes does not result in a major defect in bone resorption, further reinforcing the current emphasis placed on CTSK/Ctsk-mediated collagenolysis of the bone ECM (*16*, *17*). However, when we performed unbiased transcriptional profiling of gene expression changes occurring during the mouse macrophage-to-osteoclast transition, we noted that two MMPs—the secreted proteinase, Mmp9, and the membrane-anchored metalloproteinase, Mmp14—were tandemly up-regulated to an extent far exceeding other MMPs. Although targeting either MMP alone did not disturb osteoclast function in vitro or in vivo, we noted previously undescribed compensatory changes in gene expression between the two proteinases and unexpectedly found that simultaneous targeting of both proteinases retarded bone resorption by either mouse or human osteoclasts.

[1]The State Key Laboratory Breeding Base of Basic Science of Stomatology (Hubei-MOST) and Key Laboratory of Oral Biomedicine Ministry of Education, School and Hospital of Stomatology, Wuhan University, Wuhan 430079, China. [2]Division of Genetic Medicine, Department of Internal Medicine, University of Michigan, Ann Arbor, MI 48109, USA. [3]Life Sciences Institute, University of Michigan, Ann Arbor, MI 48109, USA. [4]Department of Pathology, Department of Urology and the Institute of Gerontology, University of Michigan, Ann Arbor, MI 48109, USA. [5]School of Dentistry, University of Michigan, Ann Arbor, MI 48109, USA.
*Corresponding author. Email: lingxin.zhu@whu.edu.cn (L.Z.); sjweiss@umich.edu (S.J.W.)

In vivo, *Mmp9*/conditional *Mmp14* double-knockout (DKO) mice had reduced homeostatic bone turnover and were protected from pathologic bone loss. Together, these studies characterize a two-partner, MMP-dependent bone collagenolytic axis that serves as a critical checkpoint for osteoclast-mediated bone resorption. Tandem targeting of osteoclast MMP9 and MMP14 may, therefore, serve as a potential therapeutic strategy to control bone-wasting diseases.

RESULTS

Mouse osteoclasts selectively express *Mmp9* and *Mmp14* in vitro and in vivo

In the presence of M-CSF and RANKL, mouse BMDMs undergo transformation into multinucleated, tartrate-resistant acid phosphatase–positive ($TRAP^+$) osteoclasts within a 4- to 5-day culture period (*18*, *19*). To monitor the changes in MMP expression that characterize the macrophage-to-osteoclast transition, we harvested RNA at days 1 to 5 for transcriptional profiling. Changes in MMP expression were largely confined to two MMP family members, the secreted proteinase *Mmp9* and the membrane-anchored metalloenzyme *Mmp14* (Fig. 1A). Real-time polymerase chain reaction (PCR) confirmed these findings, with *Mmp9* and *Mmp14* displaying up-regulated expression in a time-dependent fashion that coincided with *Ctsk* expression (Fig. 1B). Similarly, at the protein level, both Mmp9 and Mmp14 content increased as BMDMs were induced to form osteoclasts (Fig. 1C). Using Mmp9-specific antibodies and $Mmp14^{LacZ/+}$ knock-in transgenic cells (*20*–*22*), dual patterns of Mmp9 and Mmp14 expression were localized to mature osteoclasts (Fig. 1, D to F). Extending these data in vivo using $Mmp14^{LacZ/+}$ transgenic mice in which β-galactosidase (β-gal) was engineered to include a nuclear localization signal (*20*–*22*) revealed that osteoclasts adherent to the bone surface displayed nuclear β-gal activity along with Mmp9 immunoreactivity, confirming the tandem expression of both proteinases (Fig. 1G).

Neither *Mmp9* nor *Mmp14* targeting affects osteoclast activity in vitro or in vivo

Recent studies have suggested that either Mmp9 or Mmp14 can potentially participate in osteoclast fusion programs, at least in vitro (*23*, *24*). We isolated BMDMs from $Mmp9^{-/-}$ or myeloid-specific *Mmp14* conditional knockout mice (*Csf1r-Cre*/$Mmp14^{f/f}$; hereafter referred to as $Mmp14^{\Delta M/\Delta M}$) to generate osteoclasts for functional assessment. In contrast to a recent report that used small interfering RNA (siRNA)–based knockdown of *Mmp9*, which concluded that the proteinase regulates osteoclastogenesis by trafficking to the nuclear compartment where it cleaves histone H3 (*23*), wild-type and $Mmp9^{-/-}$ osteoclasts displayed indistinguishable osteoclastogenic activity in vitro (Fig. 2A and fig. S1A) and similar, if not identical, quantities of the proteolyzed histone H3 (fig. S1B). Furthermore, when cultured atop cortical bone slices, both the wild-type and null cells comparably resorbed bone as assessed by peroxidase-conjugated wheat germ agglutinin (WGA-DAB) staining (Fig. 2B and fig. S1C) (*25*). Consistent with these in vitro findings, $Mmp9^{-/-}$ mice did not display marked changes in bone volume, trabecular number, trabecular thickness, trabecular separation, or osteoclast number (Fig. 2C and fig. S1, D and E). Serum C-terminal cross-linked type I collagen (CTX-I), a collagen degradation product generated by bone-resorbing osteoclasts (*26*), was also unaffected (fig. S1F). The overall bone length was, however, shortened by ~10% due to unrelated defects in hypertrophic ossification as described previously (fig. S1D) (*27*).

Given the morbidity and mortality displayed by *Mmp14* global null mice (*28*, *29*), $Mmp14^{\Delta M/\Delta M}$ crosses were generated to target the proteinase in myeloid progenitors, including the osteoclast-derived lineage (*30*). In contrast to earlier work describing an in vitro defect in the fusogenesis of osteoclast precursors harvested from *Mmp14* global knockout mice (*24*), osteoclasts prepared from $Mmp14^{\Delta M/\Delta M}$ mice underwent normal osteoclastogenesis and resorbed bone comparably to controls despite the near complete loss of Mmp14 expression (Fig. 2, D and E, and fig. S1, G to I). Although other studies have implicated Mmp14 in regulating the solubilization of RANKL with concomitant effects on bone resorption (*31*), bone remodeling in vivo was not perturbed in $Mmp14^{\Delta M/\Delta M}$ mice (Fig. 2F and fig. S1, J to L). In characterizing the effect of *Mmp9* or *Mmp14* targeting on osteoclast gene expression, we unexpectedly noted that the transcript and protein expression of these metalloproteinases were coregulated in a compensatory fashion. That is, when osteoclast *Mmp9* was targeted, *Mmp14*/Mmp14 was increased; conversely, targeting *Mmp14* resulted in the up-regulation of *Mmp9*/Mmp9 (Fig. 2, G and H). Together, these studies confirm that neither Mmp9 nor Mmp14 plays a major solitary role in osteoclastogenesis or bone resorption in vitro or in vivo.

Impaired bone-resorbing activity of *Mmp9*/*Mmp14* DKO osteoclasts in vitro

Because compensatory regulation between these MMPs has not been described previously, we considered that the function of these proteinases in osteoclasts might only be defined by targeting both proteinases in tandem. Hence, we generated a conditional *Mmp14*-deleted mouse model in either *Mmp9* wild-type or null backgrounds (*Csf1r-Cre*/$Mmp9^{+/+}$/$Mmp14^{f/f}$ and *Csf1r-Cre*/$Mmp9^{-/-}$/$Mmp14^{f/f}$ mice). Deletion of both *Mmp9* and *Mmp14* (herein termed DKO) did not affect the numbers of $CD11b^+$ osteoclast precursor cells recovered from harvested bone marrow or their proliferative activity (fig. S2, A and B). Osteoclastogenic induction of *Mmp9*/*Mmp14* DKO macrophages demonstrated comparable osteoclastogenesis to controls as assessed by TRAP staining and $TRAP^+$ multinucleated cell (MNC) number (Fig. 3A). When stained with phalloidin to visualize F-actin, the DKO osteoclasts were similar in size and formed a morphologically normal podosome belt on glass surfaces (Fig. 3B) (*2*). Likewise, gene expression of osteoclast markers—including *Ctsk*, *Acp5*, *Dcstamp*, *Oscar*, *Itgb3*, *Src*, and *Atp6v0d2*—was unaffected (fig. S3A), as was protein expression of osteoclast differentiation markers, including nuclear factor of activated T cells 1 (NFATc1), c-Fos, c-Src, and Ctsk (Fig. 3C) (*2*).

Given the normal pattern of differentiation in DKO osteoclasts, we next assessed their bone resorptive activity in vitro. In contrast to control osteoclasts or the single knockout osteoclasts, DKO cells displayed marked defects in both bone resorption area and bone resorption depth despite unimpaired intracellular acidification (Fig. 3, D to F, and fig. S3B). Consistent with these results, type I collagenolysis as assessed by CTX-I quantities, a marker of both Ctsk and MMP activity (*32*, *33*), was also reduced more than twofold in DKO osteoclast cultures (Fig. 3G). To exclude the possibility that defects in MMP-targeted osteoclast function arise at early stages of monocyte-to-macrophage differentiation (both *Mmp9* and *Mmp14* are deleted in bone marrow–derived myeloid cells), macrophages were prepared from $Mmp9^{-/-}$/$Mmp14^{f/f}$ mice and then transduced in vitro with a lentiviral Cre expression vector just before osteoclastogenic induction. Under these conditions, osteoclast bone resorption, but

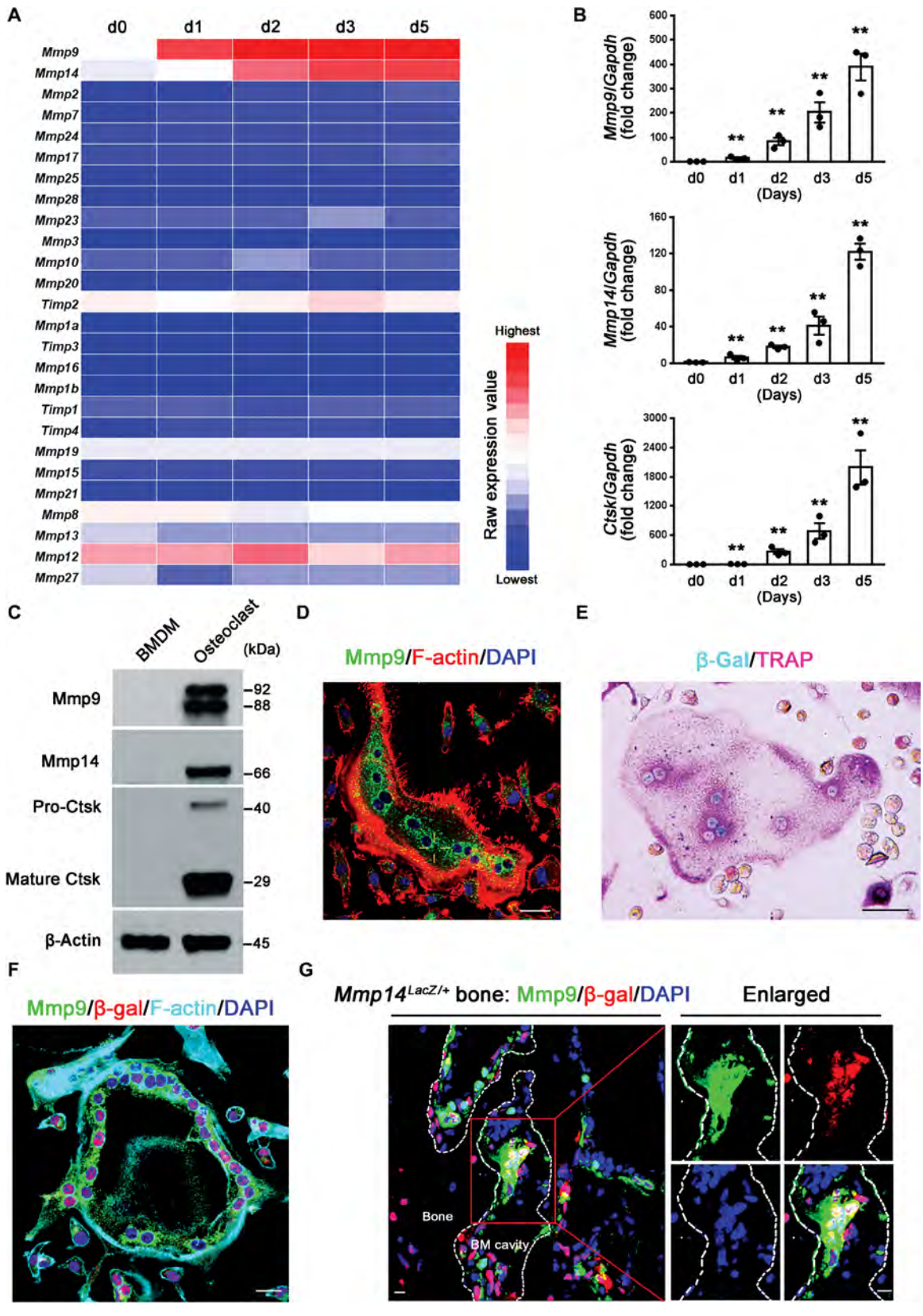

Fig. 1. Osteoclasts selectively express Mmp9 and Mmp14 in vitro and in vivo. (**A**) Transcriptional profile of MMPs and TIMPs [tissue inhibitors of metalloproteinases; (*16*, *17*)] during M-CSF/RANKL-induced differentiation of BMDMs to osteoclasts from days 0 to 5 (d0 to d5) (color bar, raw expression value). (**B**) Relative mRNA expression of *Mmp9*, *Mmp14*, and *Ctsk* during the differentiation from BMDMs to osteoclasts as a function of time in culture ($n = 3$). (**C**) Western blot of Mmp9, Mmp14, and Ctsk expression in BMDMs and mature osteoclasts. The Mmp9 doublet represents the glycosylated and nonglycosylated proforms of the proteinase (*16*, *17*). (**D**) Mmp9 (green) and F-actin (red) immunofluorescence of wild-type BMDM-derived osteoclasts. Scale bar, 20 μm. DAPI, 4′,6-diamidino-2-phenylindole. (**E**) β-gal activity (cyan) and TRAP (pink) staining of osteoclasts differentiated from $Mmp14^{LacZ/+}$ BMDMs. Scale bar, 50 μm. (**F**) Mmp9 (green), β-gal (red), and F-actin (cyan) immunofluorescence of osteoclasts differentiated from $Mmp14^{LacZ/+}$ BMDMs. Scale bar, 20 μm. (**G**) Mmp9 (green) and β-gal (red) immunofluorescence of a femur section from a $Mmp14^{LacZ/+}$ mouse. The MNCs associated with the surface of the bone marrow cavity (BM cavity) that are shown in the red box are further enlarged in the panels to the right. Scale bars, 10 μm. All results are representative of data generated in at least three independent experiments. $^{**}P < 0.01$. Error bars are means ± SEM. Data were analyzed using one-way analysis of variance (ANOVA) with Bonferroni correction.

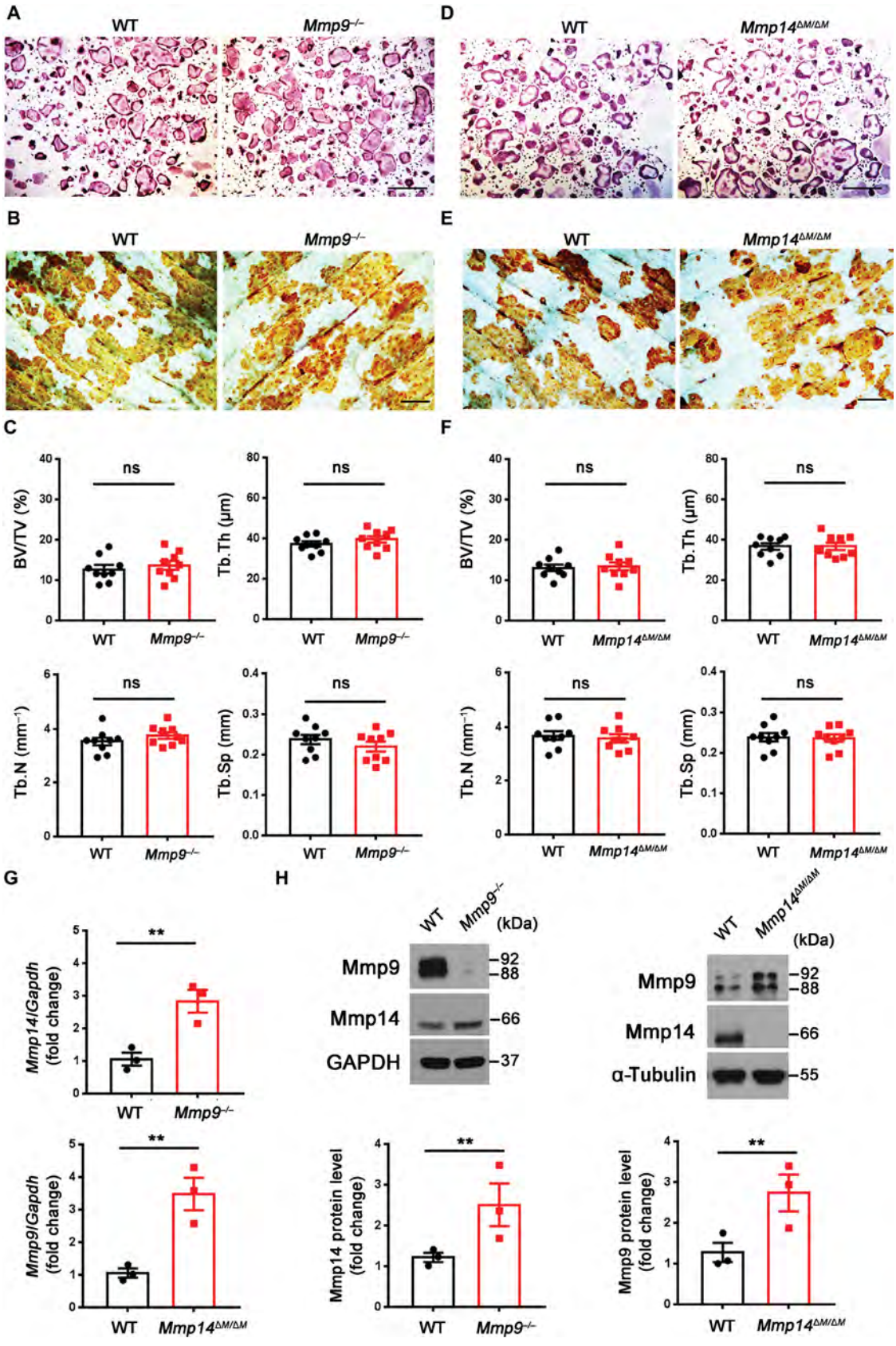

Fig. 2. *Mmp9*$^{-/-}$ and myeloid-specific *Mmp14* conditional knockout mice display normal osteoclast activity in vitro and in vivo. (**A**) BMDMs were isolated from wild-type (WT) or *Mmp9*$^{-/-}$ mice, cultured on plastic substrata with M-CSF and RANKL for 5 days, and stained with TRAP. Scale bar, 500 μm. (**B**) Wild-type or *Mmp9*$^{-/-}$ BMDMs were cultured atop bone slices and induced into osteoclasts for 6 days. After cell removal, resorption pits were visualized by WGA-DAB staining. Scale bar, 100 μm. (**C**) Quantification of bone volume/tissue volume (BV/TV), trabecular thickness (Tb.Th), trabecular number (Tb.N), and trabecular separation (Tb.Sp) as determined by μCT of 5-month-old wild-type and *Mmp9*$^{-/-}$ male mice ($n = 9$). (**D**) BMDMs were isolated from wild-type or *Mmp14*$^{\Delta M/\Delta M}$ mice, cultured atop plastic substrata with M-CSF and RANKL for 5 days, and stained with TRAP. Scale bar, 500 μm. (**E**) Wild-type or *Mmp14*$^{\Delta M/\Delta M}$ BMDMs were cultured atop bovine bone slices and induced into osteoclasts for 6 days. Cells were removed and resorption pits visualized by WGA-DAB staining. Scale bar, 100 μm. (**F**) Quantification of BV/TV, Tb.Th, Tb.N, and Tb.Sp as determined by μCT of 5-month-old wild-type and *Mmp14*$^{\Delta M/\Delta M}$ male mice ($n = 9$). (**G**) Relative mRNA expression of *Mmp14* or *Mmp9* in osteoclasts differentiated from *Mmp9*$^{-/-}$ or *Mmp14*$^{\Delta M/\Delta M}$ BMDMs ($n = 3$). (**H**) Western blot and quantification of Mmp9 and Mmp14 expression in osteoclasts differentiated from *Mmp9*$^{-/-}$ or *Mmp14*$^{\Delta M/\Delta M}$ BMDMs ($n = 3$). All results are representative of data generated in at least three independent experiments. ns, not significant. $^{**}P < 0.01$. Error bars are means ± SEM. All data were analyzed using unpaired Student's *t* test. GAPDH, glyceraldehyde-3-phosphate dehydrogenase.

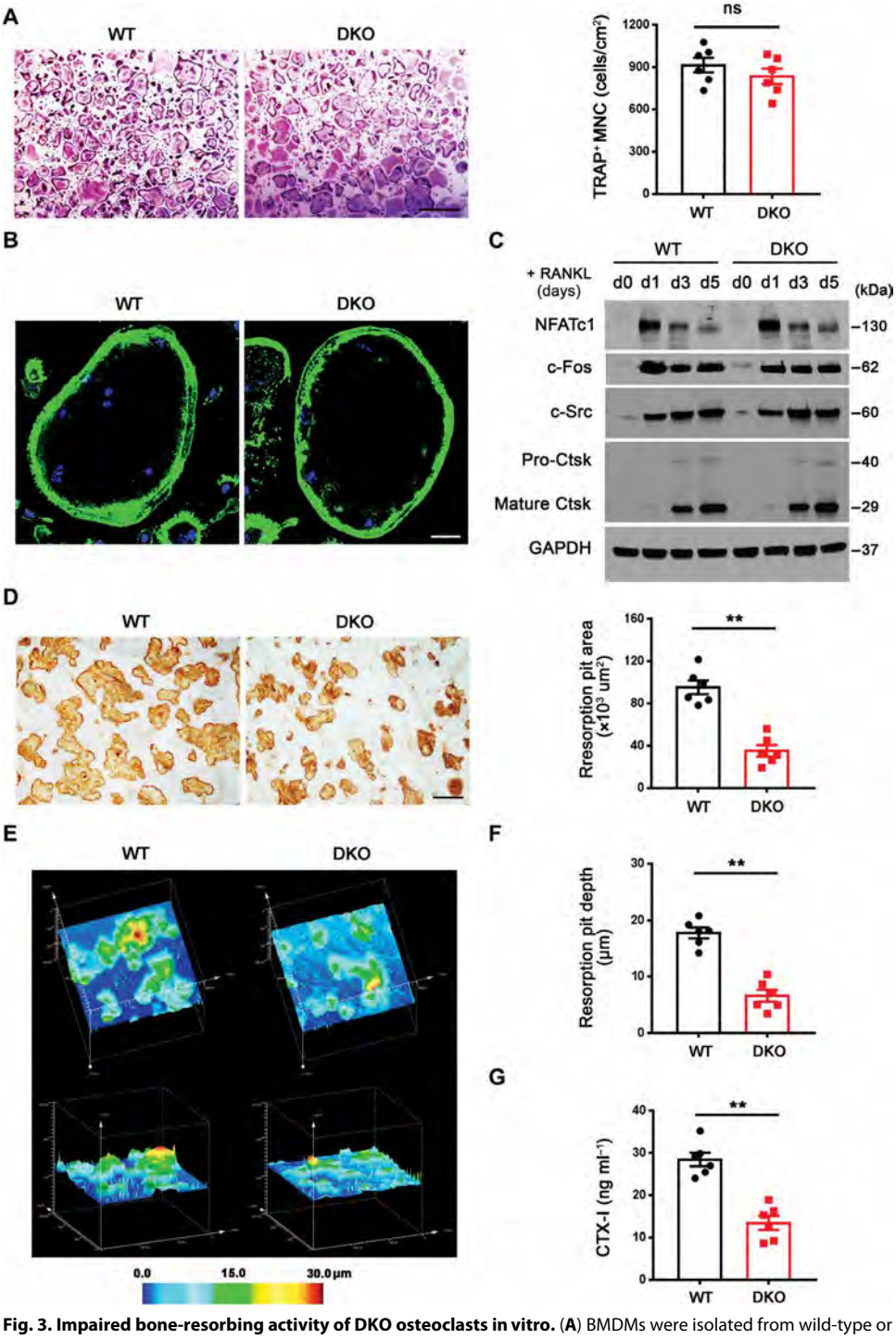

Fig. 3. Impaired bone-resorbing activity of DKO osteoclasts in vitro. (**A**) BMDMs were isolated from wild-type or DKO mice, cultured on plastic substrata with M-CSF and RANKL for 5 days, and stained with TRAP, and the number of $TRAP^+$ MNCs was determined ($n = 6$). Scale bar, 500 μm. (**B**) Phalloidin (green) staining of F-actin in wild-type or DKO osteoclasts cultured on glass. Scale bar, 20 μm. (**C**) NFATc1, c-Fos, c-Src, and Ctsk expression as assessed by Western blot in BMDMs during osteoclast differentiation. (**D**) After a 6-day culture period, wild-type or DKO osteoclasts were removed from bone slices, resorption pits were visualized by WGA-DAB staining, and resorption pit area was quantified ($n = 6$). Scale bar, 100 μm. (**E** and **F**) Resorption pits were three-dimensionally reconstructed by reflective confocal laser scanning microscope (E) in tandem with (F) quantification of resorption pit depth ($n = 6$). Color bar, pit depth. (**G**) Supernatant CTX-I was determined using ELISA ($n = 6$). All results are representative of data generated in at least three independent experiments. $^{**}P < 0.01$. Error bars are means ± SEM. All data were analyzed using unpaired Student's *t* test.

not osteoclastogenesis, was again inhibited (fig. S4, A to C). Last, whereas neutralizing monoclonal antibodies (mAbs) directed against either Mmp9 or Mmp14 alone did not affect bone resorption, the combination of both antibodies significantly inhibited resorption pit area ($^{**}P < 0.01$; fig. S4, D and E). Hence, Mmp9 and Mmp14 play compensatory, but required, late-stage roles in supporting osteoclastic bone resorption in vitro.

Mmp9 and Mmp14 catalytic activities define osteoclast-mediated bone resorption

Recent studies have assigned both proteolytic and nonproteolytic functions to MMPs (*21*, *34*–*36*). Hence, we next sought to determine whether Mmp9 or Mmp14 modulates osteoclast function in either a proteinase-dependent or -independent manner. First, using DKO osteoclasts, we transduced the cells with lentiviral expression vectors encoding either a wild-type MMP9, a catalytically inactive MMP9 point mutant [MMP9E/A (*33*)], or an empty vector (Fig. 4A). Having confirmed equivalent expression of wild-type and mutant MMP9 in the transduced cells and the ability to detect wild-type, but not catalytically inactive, MMP9 by zymography (Fig. 4B), we examined the bone-resorbing activity of the transduced cells. Lentiviral transduction of wild-type MMP9, but not MMP9E/A, fully rescued the resorption pit defects displayed by DKO osteoclasts (Fig. 4D). DKO macrophages transduced with lentiviral constructs expressing wild-type MMP14 versus the catalytically inactive MMP14 mutant, MMP14E/A (Fig. 4, A and C) (*34*), demonstrated that only wild-type MMP14 rescued bone resorption (Fig. 4E). Together, these studies indicate that an Mmp9/Mmp14 compensatory network is operative during bone resorption and is maintained by the proteolytic activities of either of the respective enzymes.

Osteoclast Mmp9 and Mmp14 exert codependent control of bone type I collagenolysis

Given that *Mmp9*/*Mmp14* DKO osteoclasts exhibit defects in collagenolytic activity and that type I collagen fragments are generated and internalized by *Ctsk*-null osteoclasts in vivo (*14*, *15*), we considered the possibility that Mmp9

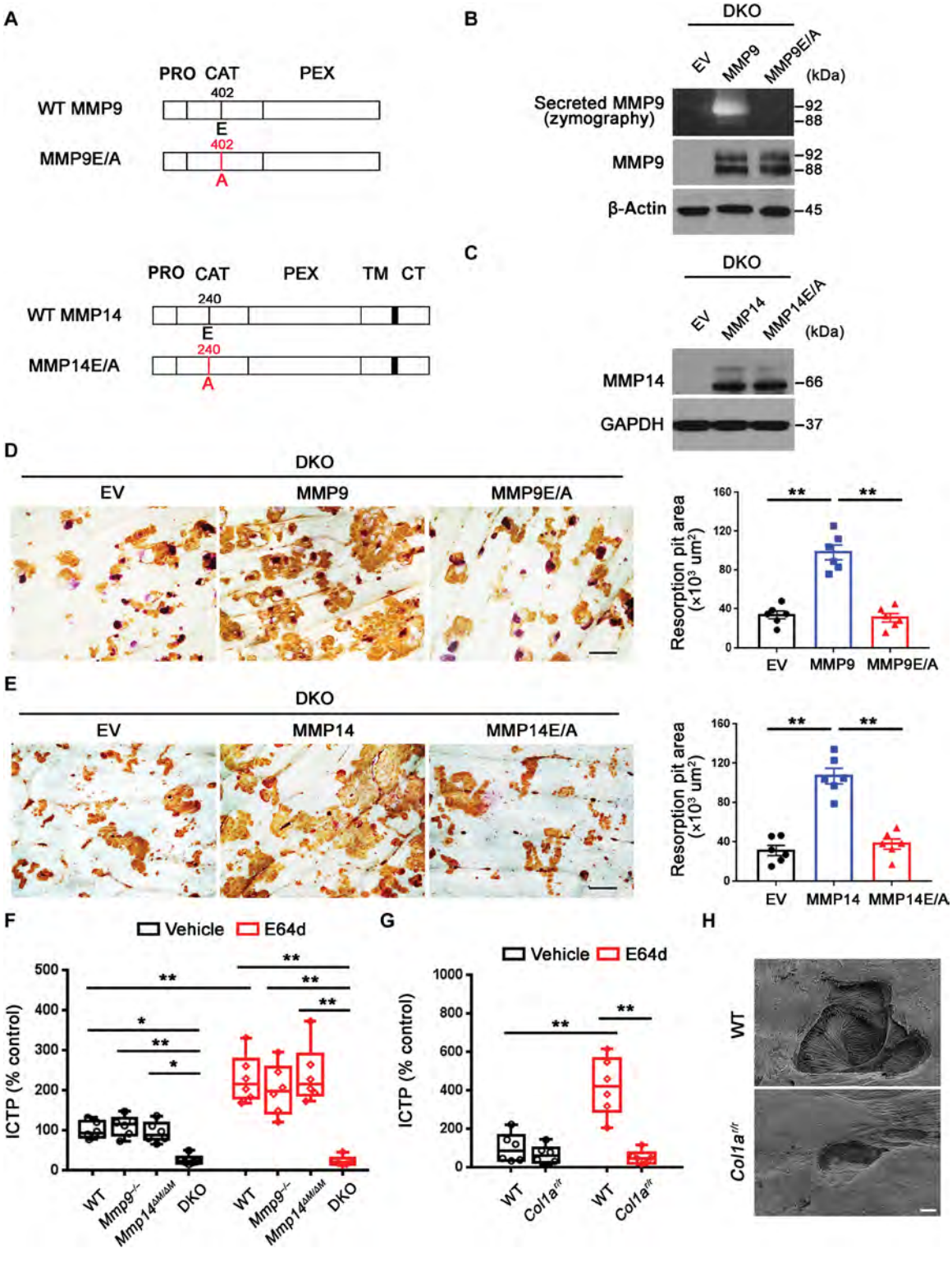

Fig. 4. Mmp9/Mmp14 catalytic activity codetermines osteoclast-mediated bone resorption by proteolyzing bone type I collagen. (**A**) A schematic diagram of full-length human MMP9 and MMP14 and their respective catalytically inactive mutants depicting the pro (PRO), catalytic (CAT), hemopexin (HPX), transmembrane (TM) domains, and cytosolic tail (CT). (**B**) DKO BMDMs were transduced with lentiviral vectors expressing full-length MMP9, an MMP9E/A mutant, or an empty control (EV) and differentiated into osteoclasts. Supernatant and cell lysate were collected for gelatin zymography and MMP9 immunoblots, respectively. (**C**) DKO BMDMs were transduced with lentiviral vectors expressing full-length MMP14, MMP14E/A, or an empty control (EV) and differentiated into osteoclasts. Cell lysates were collected for MMP14 immunoblotting. (**D**) MMP9 or MMP9E/A-transduced BMDMs were induced into osteoclasts and cultured atop bone slices for 3 days. Osteoclasts were removed, resorption pits were visualized by WGA-DAB staining, and resorption pit area was quantified ($n = 6$). Scale bar, 100 μm. (**E**) MMP14 or MMP14E/A-transduced BMDMs were induced into osteoclasts and cultured atop bone slices as described in (D). Resorption pits were visualized by WGA-DAB staining, and resorption pit area was quantified ($n = 6$). Scale bar, 100 μm. (**F**) Osteoclasts differentiated from wild-type, $Mmp9^{-/-}$, $Mmp14^{\Delta M/\Delta M}$, or DKO BMDMs were cultured atop decalcified cortical bone slices with or without E64d (20 μM) for 3 days, and supernatants were collected for ICTP ELISA ($n = 6$). (**G**) Wild-type osteoclasts were cultured atop normal or $Col1a^{r/r}$ mutant bone with or without E64d for 3 days, and supernatants were collected for ICTP ELISA ($n = 6$). (**H**) Resorption pits generated on normal or $Col1a^{r/r}$ bone by wild-type osteoclasts ex vivo were imaged by scanning electron microscopy. Scale bar, 10 μm. All results are representative of data generated in at least three independent experiments. $^*P < 0.05$, $^{**}P < 0.01$. Error bars are means ± SEM. Data were analyzed using one-way ANOVA (D and E) or two-way ANOVA (F and G) with Bonferroni correction.

and Mmp14 play compensatory roles in proteolyzing type I bone collagen. To assess the magnitude of Ctsk-independent collagenolytic activity, we cultured wild-type, *Mmp9*$^{-/-}$, *Mmp14*$^{\Delta M/\Delta M}$, or DKO osteoclasts atop decalcified bone slices to directly monitor bone collagen degradation independently of acidification/demineralization (*37*) and monitored collagen degradation by the release of the cross-linked C-terminal telopeptide of type I collagen (ICTP), a specific marker of MMP-dependent collagenolytic activity (*33*). As shown, solubilized ICTP fragments remained unaltered for either *Mmp9*-targeted or *Mmp14*-targeted osteoclasts relative to controls (Fig. 4F). By contrast, DKO osteoclasts were notably devoid of collagenolytic activity (Fig. 4F). Because Ctsk can proteolyze ICTP fragments to enzyme-linked immunosorbent assay (ELISA) undetectable products (*33*), the collagenolytic activity of control and MMP-targeted osteoclasts was reassessed atop decalcified bone in the presence of the pan-specific cysteine proteinase inhibitor, E64d (*33*). However, even under these conditions, the DKO osteoclasts were devoid of detectable activity (Fig. 4F).

In contrast to decalcified bone, Ctsk-dependent degradation of the ICTP fragment precludes its detection when osteoclasts are cultured atop native bone (*33*). Nevertheless, ICTP was increased in the presence of E64d when wild-type, *Mmp9*$^{-/-}$, or *Mmp14*$^{\Delta M/\Delta M}$ osteoclasts, but not DKO osteoclasts, resorbed native bone (fig. S5A). To further assess the relative contribution of Mmp9/Mmp14 to osteoclastic bone resorption versus that of Ctsk, we determined the bone-degradative activity of *Ctsk*$^{-/-}$ osteoclasts when incubated with or without function-blocking mAbs directed against mouse/human Mmp9/MMP9 and Mmp14/MMP14 (*38*–*40*). Each of the respective function-blocking antibodies efficiently abrogated active MMP9- or MMP14-mediated ICTP release from decalcified bone collagen, respectively (fig. S5B). Under these conditions, CTX-I–positive products were reduced threefold in *Ctsk*$^{-/-}$ osteoclasts, whereas the further addition of both function-blocking antibodies almost completely abrogated collagen degradation (fig. S5C). Consistent with these findings, when bone surface matrix proteins (dominated by type I collagen) were biotin-labeled (*41*), E64d-treated wild-type osteoclasts accumulated large amounts of labeled bone proteins in intracellular vesicles, as previously described (fig. S5D) (*42*). In contrast, the internalization of bone matrix proteins was almost completely abrogated in E64d-treated DKO osteoclasts (fig. S5D), a finding consistent with the conclusion that MMP-dependent collagenolysis plays a critical role in catalyzing the extracellular degradation of bone matrix proteins before their internalization and intracellular degradation (*41*, *43*, *44*).

Together, these results are consistent with the possibility that MMP9 and MMP14 play redundant roles in solubilizing bone collagen. Hence, decalcified bone slices were next incubated with either recombinant MMP9 or recombinant soluble MMP14. As predicted, each proteinase exhibited potent bone collagenolytic activity as assessed by either ICTP concentration or hydroxyproline release via a process that was inhibited completely by the pan-MMP inhibitor, BB-94 (fig. S5, E and F) (*34*). Moreover, as evidenced by Western blotting with an anti–type I collagen antibody, we observed the accumulation of bone type I collagen degradation products in supernatants recovered from decalcified bone slices after incubation with either active MMP9 or MMP14 (fig. S5G). Further confirming these results, whereas scanning electron microscopy of control decalcified bone collagen showed compact structures with parallel arrangement of collagen fiber bundles, exposure to MMP9 or MMP14 resulted in marked morphological changes, including disrupted collagen fiber alignment and patterns of surface erosion (fig. S5H).

A potential requirement for MMPs in bone type I collagen degradation is consistent with an earlier report, describing the inability of parathyroid (PTH)–stimulated osteoclasts to erode bone in type I collagen mutant mice (*Col1a*$^{r/r}$) in which a series of amino acid substitutions surrounding the consensus collagen cleavage site renders the triple-helical molecule resistant to MMP-dependent, but not Ctsk-dependent, collagenolysis (*45*, *46*). Hence, we cultured wild-type osteoclasts on normal versus *Col1a*$^{r/r}$ bone ex vivo. Whereas the ICTP fragment generated by wild-type osteoclasts cultured on normal bone accumulated in the presence of E64d, ICTP was decreased when cells were cultured atop *Col1a*$^{r/r}$ bone (Fig. 4G), a result confirmed by scanning electron microscopy analysis where only small, shallow pits were formed atop the MMP-resistant bone (Fig. 4H). Consistent with these data, micro–computed tomography (μCT) scans of *Col1a*$^{r/r}$ mice femurs confirmed an increase in the radio density of distal metaphyses and an increase in trabecular number and volume that was coupled with a sharp decrease in trabecular separation (fig. S6, A to E).

MMP9 and MMP14 activity controls human osteoclast-dependent bone resorption

Mouse and human monocyte-derived populations share functional characteristics; however, important distinctions also exist (*47*), raising the question of the relevance of the mouse osteoclast *Mmp9*/*Mmp14* axis to human osteoclasts. Hence, human osteoclasts were prepared from primary human CD14$^+$ monocytes (*48*). Human CD14$^+$ monocytes were induced into macrophages in the presence of M-CSF for 6 days before undergoing osteoclast differentiation in the presence of M-CSF and RANKL for an additional 9-day period (*48*). At this point, TRAP$^+$ MNCs are observed (Fig. 5, A and B). In tandem fashion, CTSK expression was induced along with MMP9 and MMP14 at both the mRNA and protein levels (Fig. 5, C and D). To assess functional requirements for MMP9 and MMP14 in supporting osteoclast activity, we cultured human osteoclasts atop bone slices in the presence of function-blocking mAbs directed against either MMP9 or MMP14 (*38*–*40*). In the presence of either the MMP9 or MMP14 mAbs alone, osteoclastogenesis proceeded in normal fashion with the unaltered formation of podosome belts (Fig. 5E). Similarly, human osteoclasts effectively degraded bone in the presence of either the anti-MMP9 or anti-MMP14 function-blocking mAbs (Fig. 5, F and G). However, when the function-blocking antibodies were used in combination, bone resorption was significantly inhibited (**$P < 0.01$; Fig. 5, F and G). Furthermore, in the presence of E64d, the combination of MMP9 and MMP14 function-blocking antibodies markedly impaired collagenolytic activity of human osteoclasts as reflected by the release of ICTP fragments (Fig. 5H). Hence, human osteoclasts, like their mouse counterparts, mobilize MMP9/MMP14 activities as a critical effector of the bone resorptive phenotype.

Mmp9/*Mmp14* DKO mice exhibit an osteopetrotic phenotype with decreased osteoclast activity in vivo

Having established that *Mmp9*/*Mmp14* deficiency affects bone collagen degradation and osteoclastic bone resorption in vitro, we sought to determine the effect of MMP targeting in vivo. We assessed bone morphometry in 5-month-old wild-type, *Mmp9*$^{-/-}$, *Mmp14*$^{\Delta M/\Delta M}$, and DKO mice. In marked contrast to the normal

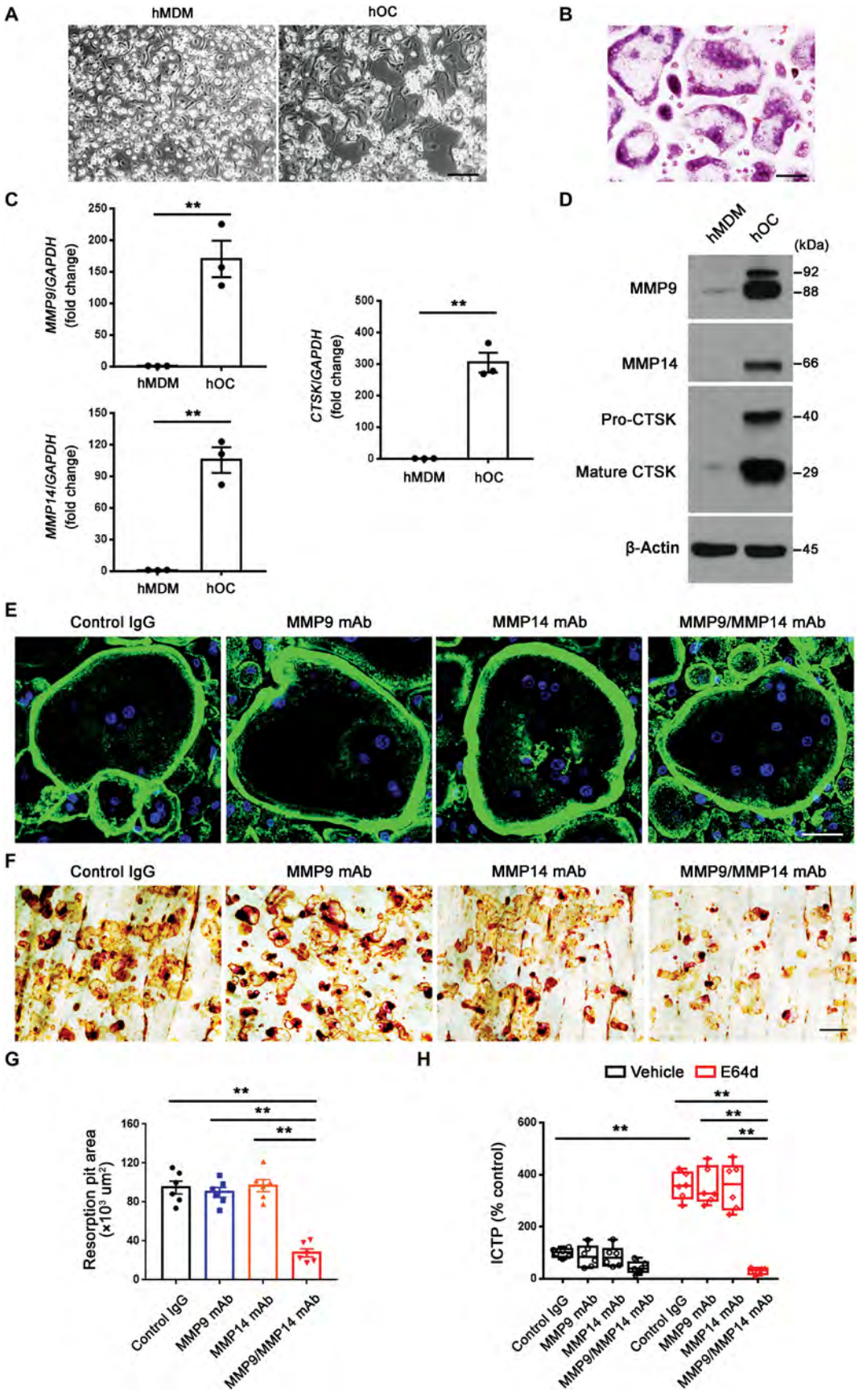

Fig. 5. Dual MMP9/MMP14 activity regulates human osteoclast-mediated bone resorption. (**A**) Phase contrast images of human monocyte-derived macrophages (hMDMs) and human osteoclasts (hOCs) differentiated from human $CD14^+$ monocytes. Scale bar, 200 μm. (**B**) TRAP staining of human osteoclasts. Scale bar, 100 μm. (**C**) Relative mRNA expression of *MMP9*, *MMP14*, and *CTSK* in hMDM and mature hOC ($n = 3$). (**D**) MMP9, MMP14, and CTSK protein expression as assessed by Western blot was determined in hMDMs and mature hOCs. (**E**) Human osteoclasts were cultured on glass in the presence or absence of an MMP9 function-blocking mAb and MMP14 function-blocking antibody (DX-2400), and the cells were stained with fluorescein isothiocyanate–phalloidin. Scale bar, 50 μm. IgG, immunoglobulin G. (**F** and **G**) Human osteoclasts were cultured atop bone slices for 6 days in the presence or absence of either the MMP9 function-blocking mAb or DX-2400. Osteoclasts were removed from the bone slices, resorption pits were visualized by (F) WGA-DAB staining, and (G) resorption pit area was quantified ($n = 6$). Scale bar, 100 μm. (**H**) Human osteoclasts were cultured atop cortical bone slices for 6 days in the presence or absence of the MMP9 or MMP14 blocking antibodies with or without E64d, and the supernatants were collected for ICTP ELISA ($n = 6$). All results are representative of data generated in at least three independent experiments. $^{**}P < 0.01$. Error bars are means ± SEM. Data were analyzed using unpaired Student's *t* test (C), one-way ANOVA (G), or two-way ANOVA (H) with Bonferroni correction.

bone seen in *Mmp9*$^{-/-}$ or *Mmp14*$^{\Delta M/\Delta M}$ mice, the dual targeting of *Mmp9* and *Mmp14* elicited a marked osteopetrotic-like effect with unusually dense trabeculation of the bone marrow spaces, resulting in a 200% increase in bone mass (Fig. 6, A to C). μCT scans of the distal femurs of male mice demonstrated that bone volume/tissue volume, number of trabeculae, and trabecular thickness were all increased,

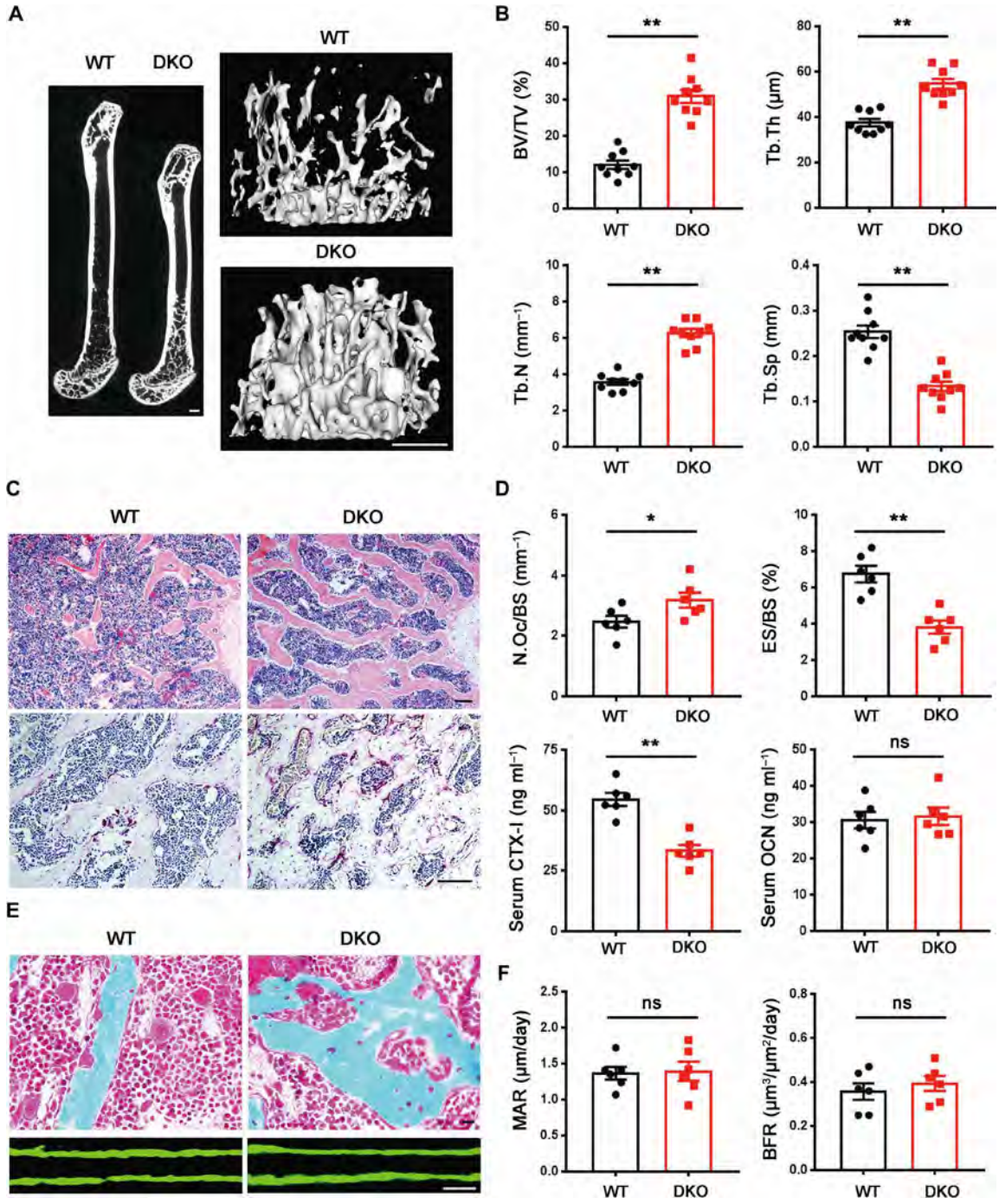

Fig. 6. DKO mice exhibit an osteopetrotic phenotype with decreased osteoclast activity. (**A**) Representative μCT of sagittal sections of femurs with three-dimensional (3D) reconstruction of the distal femur trabeculae of 5-month-old wild-type and DKO male mice is shown. Scale bars, 500 μm. (**B**) Quantification of BV/TV, Tb.Th, Tb.N, and Tb.Sp as determined by μCT in 5-month-old wild-type and DKO male mice ($n = 9$). (**C**) Hematoxylin and eosin (H&E) and TRAP staining of the distal femurs of 5-month-old male wild-type and DKO mice. Scale bars, 100 μm. (**D**) Quantification of osteoclast number per bone surface (N.Oc/BS) and eroded surface per bone surface (ES/BS) and serum CTX-I and OCN in 5-month-old wild-type and DKO male mice are shown ($n = 6$). (**E**) Golden's trichrome staining of the distal femurs of 5-month-old male wild-type and DKO mice was performed along with double calcein bone labeling and confocal imaging to assess bone formation. Scale bars, 10 μm. (**F**) Quantification of MAR and BFR as assessed in 5-month-old male wild-type and DKO mice ($n = 6$). *$P < 0.05$, **$P < 0.01$. Error bars are means ± SEM. All data were analyzed using unpaired Student's *t* test.

whereas trabecular separation was decreased relative to controls (Fig. 6B). Similar changes in cancellous bone were observed in the lumbar vertebrae of DKO mice (fig. S7, A and B). Complementing these findings, serum CTX-I fell by ~50% in the DKO mice (Fig. 6D). However, in contrast to its effects on cancellous bone, Mmp9/Mmp14 double deficiency caused a modest, but statistically significant, increase in cortical bone thickness (**$P < 0.01$; fig. S7C), a finding similar to the phenotype observed by myeloid-specific deletion of proliferator-activated receptor coactivator 1β or miR-182 (*49*, *50*). Because osteoclast activity is dispensable for growth plate resorption and bone elongation (*51*), we also note that the reduced bone length and enlarged growth plate observed in *Mmp9*$^{-/-}$ mice were not further aggravated in the DKO mice (fig. S7, D to F).

Despite the loss in bone remodeling activity, TRAP staining revealed that osteoclast numbers were slightly increased in DKO mice relative to wild type, whereas surface area of bone erosions was decreased (Fig. 6, C and D). Higher-magnification images of Goldner's trichrome staining showed that DKO mice lacked the normal gaps observed between osteoclasts and trabecular bone (Howship's lacunae) (*52*) as a consequence of reduced osteoclastic bone resorption (Fig. 6E). Defects in osteoclast function can affect osteoblast activity (*53*); however, bone formation as assessed by serum osteocalcin (OCN), mineral apposition rate (MAR), or bone formation rate (BFR) did not reveal any difference between DKO mice and control mice (Fig. 6, D to F), confirming that reduced bone resorption, rather than changes in bone formation, is responsible for the osteopetrotic-like phenotype. Furthermore, consistent with the increase in bone mass, both stiffness and elastic modulus of femurs displayed a significant increase between DKO and wild-type littermates (*$P < 0.05$), whereas ultimate load and post-yield deflection did not (fig. S7G), highlighting that improved bone quality is an inherent feature of the DKO state.

Mmp9/*Mmp14* DKO mice are protected from PTH- or ovariectomy-induced bone loss

To determine whether DKO affords mice a protected status from pathologic bone loss, we examined their response to acute stimulation. PTH, an indirect-acting bone catabolic hormone (*45*, *54*), was injected into the calvarial region of wild-type and DKO mice. PTH induced significant bone erosion in the calvariae of wild-type mice (**$P < 0.01$) but little or no bone resorption in DKO mice, although PTH increased osteoclast numbers to a comparable degree between the two groups (Fig. 7, A to D). Given the protective effect of the DKO on acute bone loss, we assessed the combined targeting strategy using a more chronic bone loss model designed to mimic postmenopausal osteoporosis, a prevalent bone pathology that develops as a result of increased osteoclast activity (*5*, *6*, *19*). Female DKO and control mice underwent ovariectomy (OVX) surgery at 12 weeks of age. By 8 weeks after OVX, whereas wild-type mice displayed significant bone loss (**$P < 0.01$), DKO mice displayed a bone-sparing phenotype, as indicated by the marked retention of bone volume/tissue volume, number of trabeculae, trabecular thickness, and trabecular separation (Fig. 8, A and B). The increase in bone mass observed in the DKO mice could have potentially blunted our ability to detect morphometric changes; however, a similar protected status was observed by monitoring bone collagen degradation. Whereas control mice responded to OVX with an ~40% increase in serum CTX-I, the DKO mice showed no change after OVX (Fig. 8C). Together, these data demonstrate that dual loss of Mmp9/Mmp14 activity confers a protective effect from OVX-induced bone loss.

DISCUSSION

More than 20 years ago, the importance of *CTSK* in regulating human osteoclast activity was confirmed with its identification as the mutant gene responsible for pycnodysostosis, a hereditary bone disorder characterized by major defects in bone resorption (*11*, *12*, *55*, *56*). However, despite postnatal growth retardation, humans with pycnodysostosis, as well as *Ctsk* knockout mice, continue to grow and remodel bone (*11*–*13*, *55*, *56*). While remaining undefined, compensatory proteolytic systems have been presumed to be up-regulated in *Ctsk*-null states (*12*, *57*, *58*). Our findings, however, alternatively support the existence of a complementary, rather than up-regulated, set of proteolytic enzymes that function in tandem with CTSK/Ctsk during bone resorption. Using knockout mouse models that target both Mmp9 and Mmp14, we have uncovered a previously unrecognized proteolytic axis that functions as a critical effector of osteoclast activation and bone resorption in both physiologic and pathologic states while leaving bone formation intact.

Recent studies have implicated Mmp9 and Mmp14 in osteoclastogenesis rather than bone resorption per se, albeit by distinct mechanisms (*23*, *24*). Regarding Mmp9, Kim *et al.* (*23*) proposed that the metalloproteinase traffics to the nuclear compartment where it cleaves histone HSK18-Q19, thereby promoting osteoclastogenic gene activation. In turn, when *Mmp9* was siRNA targeted in a mouse osteoclast precursor cell line, osteoclastogenesis was almost completely inhibited (*23*). However, earlier studies of adult *Mmp9*$^{-/-}$ mice revealed no major effects on adult bone mass or osteoclast number, despite exhibiting an expanded zone of hypertrophic chondrocytes during infancy (*27*, *59*, *60*). Consistent with these studies, our data indicate that *Mmp9*-null osteoclast fusion and function are likewise unaffected in vitro or in vivo. Independent of these studies, Gonzalo *et al.* (*24*) recently reported that Mmp14 regulates myeloid cell fusion during osteoclast formation by a mechanism that operates independently of the enzyme's catalytic activity. However, earlier studies using *Mmp14*$^{-/-}$ mice do not support a major role for Mmp14 in osteoclast formation, neither in vitro nor in vivo (*28*, *31*). These issues notwithstanding, *Mmp14*$^{-/-}$ mice suffer from multiple, and ultimately fatal, organ defects affecting bone, vasculature, skeletal muscle, and adipose tissue functions that complicate efforts to directly assess osteoclast function (*21*, *22*, *28*, *29*, *61*–*63*). Mmp14 also exerts profound effects on the bone marrow environment itself by controlling skeletal stem cell function, raising the possibility that bone marrow–derived myeloid cells recovered from global knockout mice might be affected in a noncell autonomous fashion (*21*, *62*, *64*). In this regard, using myeloid-specific conditional knockout mice, we found that targeting *Mmp14* alone did not affect osteoclast differentiation or bone resorption in vitro or in vivo.

Because prior studies had not established overlapping roles for Mmp9 and Mmp14 in cell function, we initially assumed that the lack of an observed effect after the targeting of either proteinase alone indicated that the Ctsk-independent collagenolytic activity of osteoclasts likely resides in a proteolytic system that operates outside of the MMP family. However, having noted the compensatory changes between Mmp9 and Mmp14 after their respective targeting, we considered the possibility that either proteinase might support osteoclast function. As predicted, dual targeting of *Mmp9* and *Mmp14* undermined osteoclast-mediated bone resorption: DKO mice displayed notable increases in bone mass. Although *Csf1r-Cre* expression extends beyond osteoclasts to include a number of myeloid cell–derived cell populations (*30*, *65*, *66*), each of the defects we

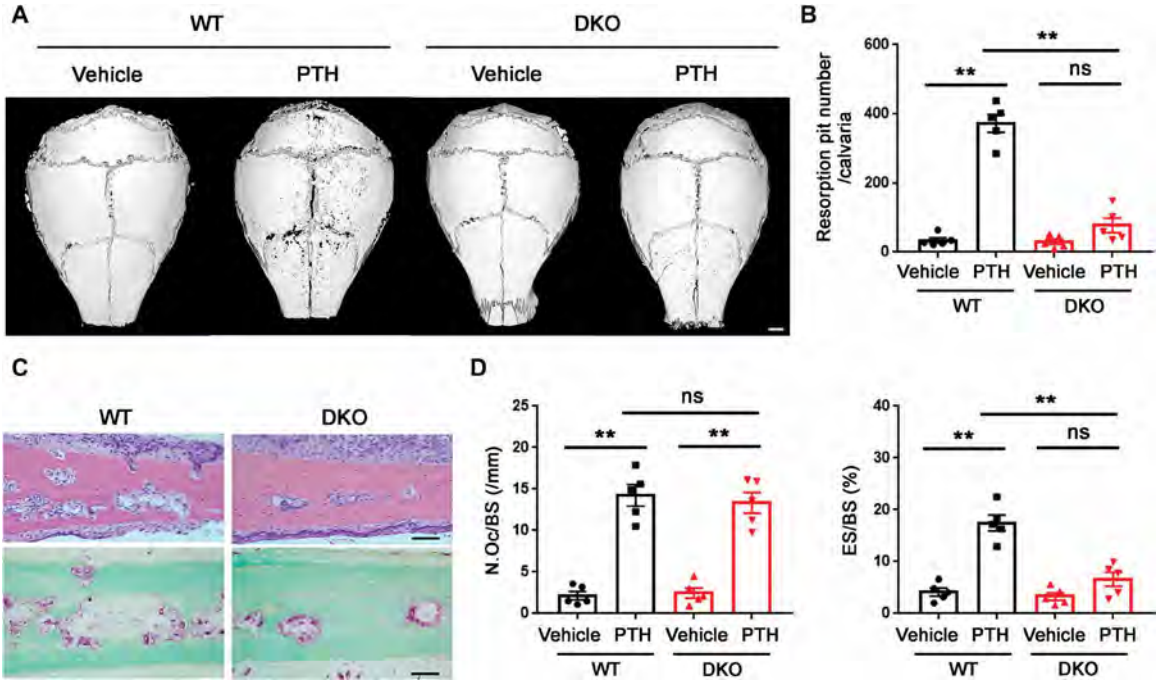

Fig. 7. PTH-induced calvarial bone erosion is alleviated in DKO mice. (**A**) Representative μCT of 3D reconstructed images of calvaria from 3-month-old male wild-type or DKO mice injected with PTH or vehicle control. Scale bar, 1000 μm. (**B**) Quantification of resorption pit number per calvaria of 3-month-old male wild-type or DKO mice injected with PTH or vehicle control ($n = 5$). (**C**) H&E and TRAP staining of calvaria from 3-month-old male wild-type or DKO mice injected with PTH. Scale bars, 50 μm. (**D**) Quantification of N.Oc/BS and ES/BS of calvaria from 3-month-old male wild-type or DKO mice injected with PTH or vehicle control ($n = 5$). $^{**}P < 0.01$. Error bars are means ± SEM. All data were analyzed using two-way ANOVA with Bonferroni correction.

observed in the targeted mice was duplicated by targeting the proteinases in vitro, both at the transcriptional and protein levels.

Several issues require consideration regarding the potential mechanisms by which osteoclast-derived Mmp9 and Mmp14 jointly participate in bone resorption. First, although our group and others have identified nonproteolytic functions for MMPs, including Mmp14 (*34*–*36*, *67*), here, we found that only the proteolytically active forms of the enzymes supported osteoclast-mediated bone resorption. Second, whereas Mmp14 functions as a collagenase by hydrolyzing acid-soluble type I collagen within its triple-helical domain (*21*, *22*, *68*), Mmp9 has not been reported to exhibit similar activity (*16*, *69*). However, although largely overlooked, in a cell-free system, Mmp9 was previously reported to depolymerize the type I collagen networks found in decalcified bone, presumably by cleaving the nonhelical telopeptide domains that contain the covalent cross-links that maintain the type I collagen fibrillar network (*32*, *70*). In this regard, a requirement for Mmp9/Mmp14 in type I collagen degradation is consistent with an earlier study describing the inability of osteoclasts to degrade mutant type I collagen that is resistant to MMP-dependent, but not Ctsk-mediated, collagenolysis (*45*, *46*). MMPs are generally believed to operate solely at neutral pH, whereas the osteoclast resorption pit is widely assumed to maintain a constant acidic pH (*17*). However, MMPs retain considerable activity even under acidic conditions (*17*, *70*), raising the possibility that these enzymes work in tandem with Ctsk in the lacunar environment. In addition, alkaline shifts have been predicted to occur within the osteoclast-bone matrix interface during the demineralization process (*3*). Last, bone lining cells have been reported to infiltrate demineralized pits left by dysfunctional osteoclasts to "rescue" bone resorption defects by deploying uncharacterized MMPs to remove undigested, exposed collagen networks (*52*, *71*). However, because osteoclasts coexpress Mmp9 and Mmp14 and both of these proteinases can directly solubilize bone collagen, the most parsimonious explanation points to osteoclast-derived Mmp9/Mmp14 as the key players in bone resorption. This conclusion is also consistent with the observation that human and mouse *Ctsk*-null osteoclasts are laden with type I collagen fibrils in vivo, despite the fact that intact cross-linked collagen cannot be internalized without undergoing extracellular proteolysis (*41*, *43*, *44*, *72*). It seems unlikely that these two MMP family members restrict their activities to collagen degradation alone. Both proteinases target a multiplicity of substrates, and further study is required to identify the full range of hydrolyzeable targets and their effects on osteoclast function. Because dual targeting of these proteinases did not affect osteoclastogenesis nor interfere with the expression of key osteoclast differentiation or functional markers, the major defects observed in bone resorption, coupled with the ability of either MMP to remodel bone collagen, support the bone collagenolytic activity of Mmp9/MMP9 and Mmp14/MMP14 as key regulators of mouse/human osteoclast activity.

To define potential therapeutic implications of targeting *Mmp9* and *Mmp14*, we used to two models of pathologic bone remodeling: PTH- and OVX-induced pathologic bone loss. Chronically high PTH encountered in primary hyperparathyroidism or as a secondary response to calcium deficiency can promote bone loss (*45*, *54*). By contrast, OVX induces bone loss secondary to the loss of estrogen that normally occurs in the postmenopausal state (*5*, *6*, *19*). MMP9 and MMP14 have been individually reported to correlate

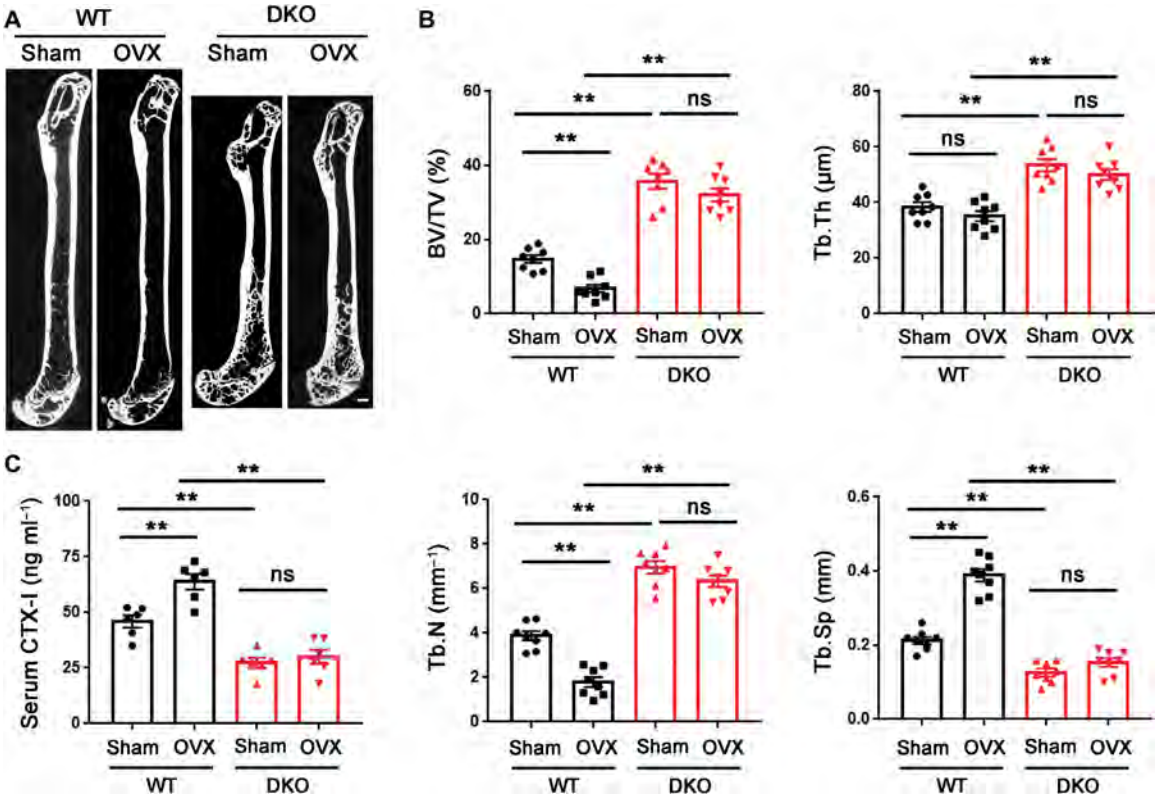

Fig. 8. DKO mice are protected from OVX-induced osteoporosis. (**A**) Representative μCT sagittal sections of femur recovered from 5-month-old female wild-type or DKO mice that underwent either sham or OVX surgery at 3 months of age. Scale bar, 500 μm. (**B**) BV/TV, Tb.Th, Tb.N, and Tb.Sp were determined by μCT of femurs from sham or OVX surgery mice ($n = 8$). (**C**) Serum CTX-I of sham or OVX surgery mice determined using ELISA ($n = 8$). $^{**}P < 0.01$. Error bars are means ± SEM. All data were analyzed using two-way ANOVA with Bonferroni correction.

with human osteoporosis status (*73*, *74*). Despite the distinct initiating mechanisms that control these two bone-resorptive states, dual targeting of *Mmp9* and *Mmp14* exerted potent bone-sparing effects in both models. Earlier work suggested that calvaria-associated osteoclasts preferentially rely on uncharacterized MMPs, as opposed to osteoclasts found in long bones where cysteine proteinase–linked mechanisms appeared to dominate (*75*). However, in our studies, bone resorption occurring in both calvaria after PTH injection and in long bones after OVX was inhibited after *Mmp9*/*Mmp14* targeting.

We showed that the roles for Mmp9/Mmp14 identified in mouse osteoclasts extended to their human counterparts and that function-blocking antibodies could attenuate bone resorption. Thus, the possibility of using these findings to design therapeutic interventions deserves consideration. Many classic antiresorptive therapies act by reducing osteoclast abundance, which compromises bone formation by affecting the bone coupling process (*5*, *6*, *76*). By contrast, Ctsk-targeted osteoclasts have been reported to maintain normal bone formation by multiple mechanisms, including elevated platelet-derived growth factor-BB and sphingosine 1-phosphate expression and protecting pro-osteoblastogenic factors from Ctsk-mediated proteolytic inactivation (*77*–*80*). Here, the double deficiency of Mmp9 and Mmp14 decreased osteoclastic bone resorption without affecting osteoclast number, thereby maintaining normal osteoblastic bone formation. Although the mechanisms maintaining normal bone formation remain to be determined, processes similar to those operative in CTSK/Ctsk-targeted osteoclasts seem likely. Recombinant humanized mAbs have been generated that effectively inhibit either human MMP9 or MMP14 (*39*, *40*, *81*). In the case of anti-human MMP9 antibodies, phase 2 clinical trials indicate that the drug is well tolerated (*81*). However, a limitation of the current study includes the potential deleterious effects of Mmp14 targeting. In this regard, Mmp14 distinguishes itself from all other MMPs as the only family member whose global deletion in mice results in early postnatal death (*28*, *29*). However, preclinical studies with function-blocking antibodies directed against Mmp14 in postnatal mice did not result in toxicity (*39*). Second caution must be exercised in extending mouse studies to the human population. For example, highly selective Ctsk inhibitors proved effective in preclinical studies, but human trials were terminated when unanticipated side effects emerged (*9*, *10*). The effect of combining selective MMP9 and MMP14 inhibitors in humans is currently unknown; efforts to inhibit their catalytic activity with function-blocking antibodies or target the yet-to-be-defined upstream cascades that regulate their expression could prove efficacious.

MATERIALS AND METHODS

Study design

This study was performed to evaluate the relative roles of Mmp9 and Mmp14 in regulating osteoclast function and the physiological and pathological consequences of their targeting on bone homeostasis. These objectives were addressed by (i) determining the MMP profile

selectively expressed in mouse osteoclasts in vitro and in vivo, (ii) characterizing the cooperative role of Mmp9/Mmp14 in controlling bone resorption and type I collagenolysis by mouse osteoclasts in vitro, (iii) demonstrating the utility of dual MMP9 and MMP14 blockade in regulating human osteoclast-dependent bone resorption, and (iv) defining the cooperative role of Mmp9/Mmp14 in controlling mouse osteoclast-dependent bone resorption during physiologic versus pathologic bone resorption in vivo. All data presented here have been replicated in independent cohorts of three or more mice or in three or more biological replicates for in vitro experiments. Samples were assigned randomly to the experimental groups. Data collection for each experiment is detailed in the respective figures, figure legends, and methods. For genotyping primers and quantitative real-time PCR primers, see tables S1 and S2, respectively. Individual subject-level data for experiments where $n < 20$ are included in data file S1. Full images of Western blots are presented in data file S2.

Statistical analysis

All values were expressed as means ± SEM. Unpaired Student's *t* test was used to analyze the differences between two groups, whereas one- or two-way analysis of variance (ANOVA) with Bonferroni correction was used to evaluate differences among multiple comparisons. $P < 0.05$ was considered statistically significant. All representative experiments shown were repeated three or more times.

SUPPLEMENTARY MATERIALS

stm.sciencemag.org/cgi/content/full/12/529/eaaw6143/DC1
Materials and Methods
Fig. S1. *Mmp9*$^{-/-}$ and myeloid-specific *Mmp14* conditional knockout mice display normal osteoclast activity in vitro and in vivo.
Fig. S2. Characterization of *Mmp9*/*Mmp14* DKO osteoclast precursors.
Fig. S3. *Mmp9*/*Mmp14* DKO osteoclasts display normal osteoclastogenesis, gene expression, and intracellular acidification.
Fig. S4. Temporal requirements for Mmp9 and Mmp14 in supporting osteoclast function.
Fig. S5. Osteoclast Mmp9/Mmp14 activities codetermine bone type I collagenolysis.
Fig. S6. *Col1a*$^{r/r}$ mutant mice exhibit an osteopetrotic phenotype in vivo.
Fig. S7. *Mmp9*/*Mmp14* DKO mice exhibit increased bone mass in lumbar vertebrae and display improved biomechanical properties.
Table S1. Genotyping PCR primers.
Table S2. Quantitative real-time PCR primers.
Data file S1. Individual subject-level data.
Data file S2. Western blotting films.
References (*82*–*89*)

View/request a protocol for this paper from *Bio-protocol*.

REFERENCES AND NOTES

1. M. Zaidi, Skeletal remodeling in health and disease. *Nat. Med.* **13**, 791–801 (2007).
2. S. L. Teitelbaum, F. P. Ross, Genetic regulation of osteoclast development and function. *Nat. Rev. Genet.* **4**, 638–649 (2003).
3. W. J. Boyle, W. S. Simonet, D. L. Lacey, Osteoclast differentiation and activation. *Nature* **423**, 337–342 (2003).
4. H. Takayanagi, Osteoimmunology: Shared mechanisms and crosstalk between the immune and bone systems. *Nat. Rev. Immunol.* **7**, 292–304 (2007).
5. T. D. Rachner, S. Khosla, L. C. Hofbauer, Osteoporosis: Now and the future. *Lancet* **377**, 1276–1287 (2011).
6. S. Khosla, L. C. Hofbauer, Osteoporosis treatment: Recent developments and ongoing challenges. *Lancet Diabetes Endocrinol.* **5**, 898–907 (2017).
7. A. G. Costa, N. E. Cusano, B. C. Silva, S. Cremers, J. P. Bilezikian, Cathepsin K: Its skeletal actions and role as a therapeutic target in osteoporosis. *Nat. Rev. Rheumatol.* **7**, 447–456 (2011).
8. M. Novinec, B. Lenarčič, Cathepsin K: A unique collagenolytic cysteine peptidase. *Biol. Chem.* **394**, 1163–1179 (2013).
9. M. T. Drake, B. L. Clarke, M. J. Oursler, S. Khosla, Cathepsin K inhibitors for osteoporosis: Biology, potential clinical utility, and lessons learned. *Endocr. Rev.* **38**, 325–350 (2017).
10. D. Brömme, P. Panwar, S. Turan, Cathepsin K osteoporosis trials, pycnodysostosis and mouse deficiency models: Commonalities and differences. *Expert Opin. Drug Discov.* **11**, 457–472 (2016).
11. B. D. Gelb, G.-P. Shi, H. A. Chapman, R. J. Desnick, Pycnodysostosis, a lysosomal disease caused by cathepsin K deficiency. *Science* **273**, 1236–1238 (1996).
12. Y. Nishi, L. Atley, D. E. Eyre, J. G. Edelson, A. Superti-Furga, T. Yasuda, R. J. Desnick, B. D. Gelb, Determination of bone markers in pycnodysostosis: Effects of cathepsin K deficiency on bone matrix degradation. *J. Bone Miner. Res.* **14**, 1902–1908 (1999).
13. P. Saftig, E. Hunziker, O. Wehmeyer, S. Jones, A. Boyde, W. Rommerskirch, J. D. Moritz, P. Schu, K. von Figura, Impaired osteoclastic bone resorption leads to osteopetrosis in cathepsin-K-deficient mice. *Proc. Natl. Acad. Sci. U.S.A.* **95**, 13453–13458 (1998).
14. V. Everts, D. C. Aronson, W. Beertsen, Phagocytosis of bone collagen by osteoclasts in two cases of pycnodysostosis. *Calcif. Tissue Int.* **37**, 25–31 (1985).
15. V. Everts, W. S. Hou, X. Rialland, W. Tigchelaar, P. Saftig, D. Brömme, B. D. Gelb, W. Beertsen, Cathepsin K deficiency in pycnodysostosis results in accumulation of non-digested phagocytosed collagen in fibroblasts. *Calcif. Tissue Int.* **73**, 380–386 (2003).
16. C. Bonnans, J. Chou, Z. Werb, Remodelling the extracellular matrix in development and disease. *Nat. Rev. Mol. Cell Biol.* **15**, 786–801 (2014).
17. K. B. S. Paiva, J. M. Granjeiro, Matrix metalloproteinases in bone resorption, remodeling, and repair. *Prog. Mol. Biol. Transl. Sci.* **148**, 203–303 (2017).
18. Y. Tang, X. Wu, W. Lei, L. Pang, C. Wan, Z. Shi, L. Zhao, T. R. Nagy, X. Peng, J. Hu, X. Feng, W. Van Hul, M. Wan, X. Cao, TGF-β1-induced migration of bone mesenchymal stem cells couples bone resorption with formation. *Nat. Med.* **15**, 757–765 (2009).
19. W. Zou, N. Rohatgi, T. H.-P. Chen, J. Schilling, Y. Abu-Amer, S. L. Teitelbaum, PPARγ regulates pharmacological but not physiological or pathological osteoclast formation. *Nat. Med.* **22**, 1203–1205 (2016).
20. I. Yana, H. Sagara, S. Takaki, K. Takatsu, K. Nakamura, K. Nakao, M. Katsuki, S.-i. Taniguchi, T. Aoki, H. Sato, S. J. Weiss, M. Seiki, Crosstalk between neovessels and mural cells directs the site-specific expression of MT1-MMP to endothelial tip cells. *J. Cell Sci.* **120**, 1607–1614 (2007).
21. Y. Tang, R. G. Rowe, E. L. Botvinick, A. Kurup, A. J. Putnam, M. Seiki, V. M. Weaver, E. T. Keller, S. Goldstein, J. Dai, D. Begun, T. Saunders, S. J. Weiss, MT1-MMP-dependent control of skeletal stem cell commitment via a β1-integrin/YAP/TAZ signaling axis. *Dev. Cell* **25**, 402–416 (2013).
22. T. Y. Feinberg, H. Zheng, R. Liu, M. S. Wicha, S. M. Yu, S. J. Weiss, Divergent matrix-remodeling strategies distinguish developmental from neoplastic mammary epithelial cell invasion programs. *Dev. Cell* **47**, 145–160.e6 (2018).
23. K. Kim, V. Punj, J.-M. Kim, S. Lee, T. S. Ulmer, W. Lu, J. C. Rice, W. An, MMP-9 facilitates selective proteolysis of the histone H3 tail at genes necessary for proficient osteoclastogenesis. *Genes Dev.* **30**, 208–219 (2016).
24. P. Gonzalo, M. C. Guadamillas, M. V. Hernández-Riquer, A. Pollán, A. Grande-García, R. A. Bartolomé, A. Vasanji, C. Ambrogio, R. Chiarle, J. Teixidó, J. Risteli, S. S. Apte, M. A. del Pozo, A. G. Arroyo, MT1-MMP is required for myeloid cell fusion via regulation of Rac1 signaling. *Dev. Cell* **18**, 77–89 (2010).
25. H. Zhao, Y. Ito, J. Chappel, N. W. Andrews, S. L. Teitelbaum, F. P. Ross, Synaptotagmin VII regulates bone remodeling by modulating osteoclast and osteoblast secretion. *Dev. Cell* **14**, 914–925 (2008).
26. A. K. Srivastava, S. Bhattacharyya, G. Castillo, N. Miyakoshi, S. Mohan, D. J. Baylink, Development and evaluation of C-telopeptide enzyme-linked immunoassay for measurement of bone resorption in mouse serum. *Bone* **27**, 529–533 (2000).
27. T. H. Vu, J. M. Shipley, G. Bergers, J. E. Berger, J. A. Helms, D. Hanahan, S. D. Shapiro, R. M. Senior, Z. Werb, MMP-9/gelatinase B is a key regulator of growth plate angiogenesis and apoptosis of hypertrophic chondrocytes. *Cell* **93**, 411–422 (1998).
28. K. Holmbeck, P. Bianco, J. Caterina, S. Yamada, M. Kromer, S. A. Kuznetsov, M. Mankani, P. G. Robey, A. R. Poole, I. Pidoux, J. M. Ward, H. Birkedal-Hansen, MT1-MMP-deficient mice develop dwarfism, osteopenia, arthritis, and connective tissue disease due to inadequate collagen turnover. *Cell* **99**, 81–92 (1999).
29. Z. Zhou, S. S. Apte, R. Soininen, R. Cao, G. Y. Baaklini, R. W. Rauser, J. Wang, Y. Cao, K. Tryggvason, Impaired endochondral ossification and angiogenesis in mice deficient in membrane-type matrix metalloproteinase I. *Proc. Natl. Acad. Sci. U.S.A.* **97**, 4052–4057 (2000).
30. S. L. Dallas, Y. Xie, L. A. Shiflett, Y. Ueki, Mouse Cre models for the study of bone diseases. *Curr. Osteoporos. Rep.* **16**, 466–477 (2018).
31. A. Hikita, I. Yana, H. Wakeyama, M. Nakamura, Y. Kadono, Y. Oshima, K. Nakamura, M. Seiki, S. Tanaka, Negative regulation of osteoclastogenesis by ectodomain shedding of receptor activator of NF-κB ligand. *J. Biol. Chem.* **281**, 36846–36855 (2006).
32. V. Parikka, P. Lehenkari, M.-L. Sassi, J. Halleen, J. Risteli, P. Härkönen, H. K. Väänänen, Estrogen reduces the depth of resorption pits by disturbing the organic bone matrix degradation activity of mature osteoclasts. *Endocrinology* **142**, 5371–5378 (2001).
33. P. Garnero, M. Ferreras, M. A. Karsdal, R. Nicamhlaoibh, J. Risteli, O. Borel, P. Qvist, P. D. Delmas, N. T. Foged, J. M. Delaissé, The type I collagen fragments ICTP and CTX

reveal distinct enzymatic pathways of bone collagen degradation. *J. Bone Miner. Res.* **18**, 859–867 (2003).
34. R. Shimizu-Hirota, W. Xiong, B. T. Baxter, S. L. Kunkel, I. Maillard, X.-W. Chen, F. Sabeh, R. Liu, X.-Y. Li, S. J. Weiss, MT1-MMP regulates the PI3Kδ·Mi-2/NuRD-dependent control of macrophage immune function. *Genes Dev.* **26**, 395–413 (2012).
35. J. L. Orgaz, P. Pandya, R. Dalmeida, P. Karagiannis, B. Sanchez-Laorden, A. Viros, J. Albrengues, F. O. Nestle, A. J. Ridley, C. Gaggioli, R. Marais, S. N. Karagiannis, V. Sanz-Moreno, Diverse matrix metalloproteinase functions regulate cancer amoeboid migration. *Nat. Commun.* **5**, 4255 (2014).
36. H. L. X. Wong, G. Jin, R. Cao, S. Zhang, Y. Cao, Z. Zhou, MT1-MMP sheds LYVE-1 on lymphatic endothelial cells and suppresses VEGF-C production to inhibit lymphangiogenesis. *Nat. Commun.* **7**, 10824 (2016).
37. K. Henriksen, M. G. Sørensen, R. H. Nielsen, J. Gram, S. Schaller, M. H. Dziegiel, V. Everts, J. Bollerslev, M. A. Karsdal, Degradation of the organic phase of bone by osteoclasts: A secondary role for lysosomal acidification. *J. Bone Miner. Res.* **21**, 58–66 (2006).
38. Y. Gong, E. Hart, A. Shchurin, J. Hoover-Plow, Inflammatory macrophage migration requires MMP-9 activation by plasminogen in mice. *J. Clin. Invest.* **118**, 3012–3024 (2008).
39. L. Devy, L. Huang, L. Naa, N. Yanamandra, H. Pieters, N. Frans, E. Chang, Q. Tao, M. Vanhove, A. Lejeune, R. van Gool, D. J. Sexton, G. Kuang, D. Rank, S. Hogan, C. Pazmany, Y. L. Ma, S. Schoonbroodt, A. E. Nixon, R. C. Ladner, R. Hoet, P. Henderikx, C. Tenhoor, S. A. Rabbani, M. L. Valentino, C. R. Wood, D. T. Dransfield, Selective inhibition of matrix metalloproteinase-14 blocks tumor growth, invasion, and angiogenesis. *Cancer Res.* **69**, 1517–1526 (2009).
40. E. I. Ager, S. V. Kozin, N. D. Kirkpatrick, G. Seano, D. P. Kodack, V. Askoxylakis, Y. Huang, S. Goel, M. Snuderl, A. Muzikansky, D. M. Finkelstein, D. T. Dransfield, L. Devy, Y. Boucher, D. Fukumura, R. K. Jain, Blockade of MMP14 activity in murine breast carcinomas: Implications for macrophages, vessels, and radiotherapy. *J. Natl. Cancer Inst.* **107**, djv017 (2015).
41. H. Lee, C. M. Overall, C. A. McCulloch, J. Sodek, A critical role for the membrane-type 1 matrix metalloproteinase in collagen phagocytosis. *Mol. Biol. Cell* **17**, 4812–4826 (2006).
42. P. Leung, M. Pickarski, Y. Zhuo, P. J. Masarachia, L. T. Duong, The effects of the cathepsin K inhibitor odanacatib on osteoclastic bone resorption and vesicular trafficking. *Bone* **49**, 623–635 (2011).
43. D. H. Madsen, L. H. Engelholm, S. Ingvarsen, T. Hillig, R. A. Wagenaar-Miller, L. Kjøller, H. Gårdsvoll, G. Høyer-Hansen, K. Holmbeck, T. H. Bugge, N. Behrendt, Extracellular collagenases and the endocytic receptor, urokinase plasminogen activator receptor-associated protein/Endo180, cooperate in fibroblast-mediated collagen degradation. *J. Biol. Chem.* **282**, 27037–27045 (2007).
44. R. A. Wagenaar-Miller, L. H. Engelholm, J. Gavard, S. S. Yamada, J. S. Gutkind, N. Behrendt, T. H. Bugge, K. Holmbeck, Complementary roles of intracellular and pericellular collagen degradation pathways in vivo. *Mol. Cell. Biol.* **27**, 6309–6322 (2007).
45. W. Zhao, M. H. Byrne, B. F. Boyce, S. M. Krane, Bone resorption induced by parathyroid hormone is strikingly diminished in collagenase-resistant mutant mice. *J. Clin. Invest.* **103**, 517–524 (1999).
46. P. Garnero, O. Borel, I. Byrjalsen, M. Ferreras, F. H. Drake, M. S. McQueney, N. T. Foged, P. D. Delmas, J.-M. Delaisse, The collagenolytic activity of cathepsin K is unique among mammalian proteinases. *J. Biol. Chem.* **273**, 32347–32352 (1998).
47. F. Ginhoux, S. Jung, Monocytes and macrophages: Developmental pathways and tissue homeostasis. *Nat. Rev. Immunol.* **14**, 392–404 (2014).
48. B. Raynaud-Messina, L. Bracq, M. Dupont, S. Souriant, S. M. Usmani, A. Proag, K. Pingris, V. Soldan, C. Thibault, F. Capilla, T. Al Saati, I. Gennero, P. Jurdic, P. Jolicoeur, J.-L. Davignon, T. R. Mempel, S. Benichou, I. Maridonneau-Parini, C. Vérollet, Bone degradation machinery of osteoclasts: An HIV-1 target that contributes to bone loss. *Proc. Natl. Acad. Sci. U.S.A.* **115**, E2556–E2565 (2018).
49. Y. Zhang, N. Rohatgi, D. J. Veis, J. Schilling, S. L. Teitelbaum, W. Zou, PGC1β organizes the osteoclast cytoskeleton by mitochondrial biogenesis and activation. *J. Bone Miner. Res.* **33**, 1114–1125 (2018).
50. K. Inoue, Z. Deng, Y. Chen, E. Giannopoulou, R. Xu, S. Gong, M. B. Greenblatt, L. S. Mangala, G. Lopez-Berestein, D. G. Kirsch, A. K. Sood, L. Zhao, B. Zhao, Bone protection by inhibition of microRNA-182. *Nat. Commun.* **9**, 4108 (2018).
51. S. G. Romeo, K. M. Alawi, J. Rodrigues, A. Singh, A. P. Kusumbe, S. K. Ramasamy, Endothelial proteolytic activity and interaction with non-resorbing osteoclasts mediate bone elongation. *Nat. Cell Biol.* **21**, 430–441 (2019).
52. V. Everts, J. M. Delaissé, W. Korper, D. C. Jansen, W. Tigchelaar-Gutter, P. Saftig, W. Beertsen, The bone lining cell: Its role in cleaning Howship's lacunae and initiating bone formation. *J. Bone Miner. Res.* **17**, 77–90 (2002).
53. N. A. Sims, T. J. Martin, Coupling the activities of bone formation and resorption: A multitude of signals within the basic multicellular unit. *BoneKEy Rep.* **3**, 481 (2014).
54. W. Zou, H. Kitaura, J. Reeve, F. Long, V. L. J. Tybulewicz, S. J. Shattil, M. H. Ginsberg, F. P. Ross, S. L. Teitelbaum, Syk, c-Src, the αvβ3 integrin, and ITAM immunoreceptors, in concert, regulate osteoclastic bone resorption. *J. Cell Biol.* **176**, 877–888 (2007).
55. N. Ho, A. Punturieri, D. Wilkin, J. Szabo, M. Johnson, J. Whaley, J. Davis, A. Clark, S. Weiss, C. Francomano, Mutations of CTSK result in pycnodysostosis via a reduction in cathepsin K protein. *J. Bone Miner. Res.* **14**, 1649–1653 (1999).
56. M. R. Johnson, M. H. Polymeropoulos, H. L. Vos, R. I. Ortiz de Luna, C. A. Francomano, A nonsense mutation in the cathepsin K gene observed in a family with pycnodysostosis. *Genome Res.* **6**, 1050–1055 (1996).
57. V. Everts, W. Korper, K. A. Hoeben, I. D. C. Jansen, D. Bromme, K. B. J. M. Cleutjens, S. Heeneman, C. Peters, T. Reinheckel, P. Saftig, W. Beertsen, Osteoclastic bone degradation and the role of different cysteine proteinases and matrix metalloproteinases: Differences between calvaria and long bone. *J. Bone Miner. Res.* **21**, 1399–1408 (2006).
58. M. Okaji, H. Sakai, E. Sakai, M. Shibata, F. Hashimoto, Y. Kobayashi, N. Yoshida, K. Okamoto, K. Yamamoto, Y. Kato, The regulation of bone resorption in tooth formation and eruption processes in mouse alveolar crest devoid of cathepsin k. *J. Pharmacol. Sci.* **91**, 285–294 (2003).
59. M. T. Engsig, Q.-J. Chen, T. H. Vu, A.-C. Pedersen, B. Therkidsen, L. R. Lund, K. Henriksen, T. Lenhard, N. T. Foged, Z. Werb, J.-M. Delaisse, Matrix metalloproteinase 9 and vascular endothelial growth factor are essential for osteoclast recruitment into developing long bones. *J. Cell Biol.* **151**, 879–889 (2000).
60. J. S. Nyman, C. C. Lynch, D. S. Perrien, S. Thiolloy, E. C. O'Quinn, C. A. Patil, X. Bi, G. M. Pharr, A. Mahadevan-Jansen, G. R. Mundy, Differential effects between the loss of MMP-2 and MMP-9 on structural and tissue-level properties of bone. *J. Bone Miner. Res.* **26**, 1252–1260 (2011).
61. K. M. Chan, H. L. X. Wong, G. Jin, B. Liu, R. Cao, Y. Cao, K. Lehti, K. Tryggvason, Z. Zhou, MT1-MMP inactivates ADAM9 to regulate FGFR2 signaling and calvarial osteogenesis. *Dev. Cell* **22**, 1176–1190 (2012).
62. C. Nishida, K. Kusubata, Y. Tashiro, I. Gritli, A. Sato, M. Ohki-Koizumi, Y. Morita, M. Nagano, T. Sakamoto, N. Koshikawa, T. Kuchimaru, S. Kizaka-Kondoh, M. Seiki, H. Nakauchi, B. Heissig, K. Hattori, MT1-MMP plays a critical role in hematopoiesis by regulating HIF-mediated chemokine/cytokine gene transcription within niche cells. *Blood* **119**, 5405–5416 (2012).
63. A. Gutiérrez-Fernández, C. Soria-Valles, F. G. Osorio, J. Gutiérrez-Abril, C. Garabaya, A. Aguirre, A. Fueyo, M. S. Fernández-García, X. S. Puente, C. López-Otín, Loss of MT1-MMP causes cell senescence and nuclear defects which can be reversed by retinoic acid. *EMBO J.* **34**, 1875–1888 (2015).
64. G. Jin, F. Zhang, K. M. Chan, H. L. X. Wong, B. Liu, K. S. E. Cheah, X. Liu, C. Mauch, D. Liu, Z. Zhou, MT1-MMP cleaves Dll1 to negatively regulate Notch signalling to maintain normal B-cell development. *EMBO J.* **30**, 2281–2293 (2011).
65. T. A. Wynn, A. Chawla, J. W. Pollard, Macrophage biology in development, homeostasis and disease. *Nature* **496**, 445–455 (2013).
66. A. Plein, A. Fantin, L. Denti, J. W. Pollard, C. Ruhrberg, Erythro-myeloid progenitors contribute endothelial cells to blood vessels. *Nature* **562**, 223–228 (2018).
67. T. Sakamoto, M. Seiki, Integrated functions of membrane-type 1 matrix metalloproteinase in regulating cancer malignancy: Beyond a proteinase. *Cancer Sci.* **108**, 1095–1100 (2017).
68. E. Ohuchi, K. Imai, Y. Fujii, H. Sato, M. Seiki, Y. Okada, Membrane type 1 matrix metalloproteinase digests interstitial collagens and other extracellular matrix macromolecules. *J. Biol. Chem.* **272**, 2446–2451 (1997).
69. S. K. Sarkar, B. Marmer, G. Goldberg, K. C. Neuman, Single-molecule tracking of collagenase on native type I collagen fibrils reveals degradation mechanism. *Curr. Biol.* **22**, 1047–1056 (2012).
70. Y. Okada, K. Naka, K. Kawamura, T. Matsumoto, I. Nakanishi, N. Fujimoto, H. Sato, M. Seiki, Localization of matrix metalloproteinase 9 (92-kilodalton gelatinase/type IV collagenase = gelatinase B) in osteoclasts: Implications for bone resorption. *Lab. Invest.* **72**, 311–322 (1995).
71. T. L. Andersen, M. del Carmen Ovejero, T. Kirkegaard, T. Lenhard, N. T. Foged, J.-M. Delaisse, A scrutiny of matrix metalloproteinases in osteoclasts: Evidence for heterogeneity and for the presence of MMPs synthesized by other cells. *Bone* **35**, 1107–1119 (2004).
72. V. Everts, E. van der Zee, L. Creemers, W. Beertsen, Phagocytosis and intracellular digestion of collagen, its role in turnover and remodelling. *Histochem. J.* **28**, 229–245 (1996).
73. C. E. Bolton, M. D. Stone, P. H. Edwards, J. M. Duckers, W. D. Evans, D. J. Shale, Circulating matrix metalloproteinase-9 and osteoporosis in patients with chronic obstructive pulmonary disease. *Chron. Respir. Dis.* **6**, 81–87 (2009).
74. Q.-h. Zhou, X. F. Huang, J.-h. Wang, C.-w. Lin, Y.-y. Yang, C.-s. Huang, L.-t. Wu, Y.-m. Wu, Association of MMP14 gene polymorphisms and osteoporosis in Zhuang men from Baise region of Guangxi. *Zhonghua Yi Xue Yi Chuan Xue Za Zhi* **29**, 309–313 (2012).
75. V. Everts, W. Korper, D. C. Jansen, J. Steinfort, I. Lammerse, S. Heera, A. J. P. Docherty, W. Beertsen, Functional heterogeneity of osteoclasts: Matrix metalloproteinases participate in osteoclastic resorption of calvarial bone but not in resorption of long bone. *FASEB J.* **13**, 1219–1230 (1999).

76. S. L. Teitelbaum, Therapeutic implications of suppressing osteoclast formation *versus* function. *Rheumatology (Oxford)* **55**, ii61–ii63 (2016).
77. H. Xie, Z. Cui, L. Wang, Z. Xia, Y. Hu, L. Xian, C. Li, L. Xie, J. Crane, M. Wan, G. Zhen, Q. Bian, B. Yu, W. Chang, T. Qiu, M. Pickarski, L. T. Duong, J. J. Windle, X. Luo, E. Liao, X. Cao, PDGF-BB secreted by preosteoclasts induces angiogenesis during coupling with osteogenesis. *Nat. Med.* **20**, 1270–1278 (2014).
78. S. Lotinun, R. Kiviranta, T. Matsubara, J. A. Alzate, L. Neff, A. Lüth, I. Koskivirta, B. Kleuser, J. Vacher, E. Vuorio, W. C. Horne, R. Baron, Osteoclast-specific cathepsin K deletion stimulates S1P-dependent bone formation. *J. Clin. Invest.* **123**, 666–681 (2013).
79. K. Fuller, K. M. Lawrence, J. L. Ross, U. B. Grabowska, M. Shiroo, B. Samuelsson, T. J. Chambers, Cathepsin K inhibitors prevent matrix-derived growth factor degradation by human osteoclasts. *Bone* **42**, 200–211 (2008).
80. N. Bonnet, J. Brun, J.-C. Rousseau, L. T. Duong, S. L. Ferrari, Cathepsin K controls cortical bone formation by degrading periostin. *J. Bone Miner. Res.* **32**, 1432–1441 (2017).
81. D. C. Marshall, S. K. Lyman, S. McCauley, M. Kovalenko, R. Spangler, C. Liu, M. Lee, C. O'Sullivan, V. Barry-Hamilton, H. Ghermazien, A. Mikels-Vigdal, C. A. Garcia, B. Jorgensen, A. C. Velayo, R. Wang, J. I. Adamkewicz, V. Smith, Selective allosteric inhibition of MMP9 is efficacious in preclinical models of ulcerative colitis and colorectal cancer. *PLOS ONE* **10**, e0127063 (2015).
82. Y. Tang, T. Feinberg, E. T. Keller, X.-Y. Li, S. J. Weiss, Snail/Slug binding interactions with YAP/TAZ control skeletal stem cell self-renewal and differentiation. *Nat. Cell Biol.* **18**, 917–929 (2016).
83. D. W. Dempster, J. E. Compston, M. K. Drezner, F. H. Glorieux, J. A. Kanis, H. Malluche, P. J. Meunier, S. M. Ott, R. R. Recker, A. M. Parfitt, Standardized nomenclature, symbols, and units for bone histomorphometry: A 2012 update of the report of the ASBMR Histomorphometry Nomenclature Committee. *J. Bone Miner. Res.* **28**, 2–17 (2013).
84. R. A. Irizarry, B. Hobbs, F. Collin, Y. D. Beazer-Barclay, K. J. Antonellis, U. Scherf, T. P. Speed, Exploration, normalization, and summaries of high density oligonucleotide array probe level data. *Biostatistics* **4**, 249–264 (2003).
85. W. Geng, K. Hill, J. E. Zerwekh, T. Kohler, R. Müller, O. W. Moe, Inhibition of osteoclast formation and function by bicarbonate: Role of soluble adenylyl cyclase. *J. Cell. Physiol.* **220**, 332–340 (2009).
86. F. Sabeh, I. Ota, K. Holmbeck, H. Birkedal-Hansen, P. Soloway, M. Balbin, C. Lopez-Otin, S. Shapiro, M. Inada, S. Krane, E. Allen, D. Chung, S. J. Weiss, Tumor cell traffic through the extracellular matrix is controlled by the membrane-anchored collagenase MT1-MMP. *J. Cell Biol.* **167**, 769–781 (2004).
87. S. Filippov, G. C. Koenig, T.-H. Chun, K. B. Hotary, I. Ota, T. H. Bugge, J. D. Roberts, W. P. Fay, H. Birkedal-Hansen, K. Holmbeck, F. Sabeh, E. D. Allen, S. J. Weiss, MT1-matrix metalloproteinase directs arterial wall invasion and neointima formation by vascular smooth muscle cells. *J. Exp. Med.* **202**, 663–671 (2005).
88. J. Salo, P. Lehenkari, M. Mulari, K. Metsikkö, H. K. Väänänen, Removal of osteoclast bone resorption products by transcytosis. *Science* **276**, 270–273 (1997).
89. B. P. Sinder, J. D. Salemi, M. S. Ominsky, M. S. Caird, J. C. Marini, K. M. Kozloff, Rapidly growing Brtl/+ mouse model of osteogenesis imperfecta improves bone mass and strength with sclerostin antibody treatment. *Bone* **71**, 115–123 (2015).

Acknowledgments: We thank S. L. Teitelbaum (Washington University School of Medicine in St. Louis) for sharing protocols of primary bone cell culture and helpful discussions, S. Meshinchi (University of Michigan Microscopy Core) for assistance in imaging, and C. Whitinger (Michigan Integrative Musculoskeletal Health Core Center) for assistance with bone histomorphometry. We thank the Kadmon Corporation for providing the anti-MMP14 antibody licensed to the Kadmon Corporation by the Dyax Corporation. **Funding:** This work was supported by a grant from the Breast Cancer Research Foundation (to S.J.W.). Work performed in this study was also supported by NIH grants R01-AI105068, R01-CA071699, and R01-AR075168 and the Margolies Family Discovery Fund for Cancer Research (to S.J.W.) ; P01-CA093900 (to E.T.K.); and the NSFC 81970919 (to L.Z.). Core support was provided by the National Cancer Institute of the National Institutes of Health under award number P30-AR069620. **Author contributions:** L.Z. and S.J.W. designed and supervised the project, analyzed data, wrote the manuscript, and approved the final version. L.Z., Y.T., X.-Y.L., E.T.K., J.Y., J.-S.C., and T.Y.F. performed experiments, analyzed data, and provided relevant advice. **Competing interests:** The authors declare that they have no competing interests. **Data and materials availability:** All data associated with this study are present in the paper or the Supplementary Materials. Microarray data have been deposited in the Gene Expression Omnibus (accession number GSE138324).

Submitted 5 February 2019
Resubmitted 3 October 2019
Accepted 2 January 2020
Published 5 February 2020
10.1126/scitranslmed.aaw6143

Citation: L. Zhu, Y. Tang, X.-Y. Li, E. T. Keller, J. Yang, J.-S. Cho, T. Y. Feinberg, S. J. Weiss, Osteoclast-mediated bone resorption is controlled by a compensatory network of secreted and membrane-tethered metalloproteinases. *Sci. Transl. Med.* **12**, eaaw6143 (2020).

Science Translational Medicine

Osteoclast-mediated bone resorption is controlled by a compensatory network of secreted and membrane-tethered metalloproteinases

Lingxin Zhu, Yi Tang, Xiao-Yan Li, Evan T. Keller, Jingwen Yang, Jung-Sun Cho, Tamar Y. Feinberg and Stephen J. Weiss

Sci Transl Med **12**, eaaw6143.
DOI: 10.1126/scitranslmed.aaw6143

Codependent deconstruction

Bone homeostasis encompasses a balancing act between formation of new bone and remodeling and resorption of existing bone. For patients with bone-wasting disorders such as osteoporosis, bone resorption predominates. To identify potential therapeutic targets in maladaptive bone resorption, Zhu *et al.* investigated mechanisms of collagenolytic activity in osteoclasts. They found that dual deletion of the matrix metalloproteinases MMP9 and MMP14 inhibited murine and human osteoclast activity, increased bone density, and prevented against pathogenic bone loss in mice. Dual targeting of MMP9 and MMP14 could potentially help treat bone-wasting diseases.